HYDROGEOLOGIC INVESTIGATION OF THE BELGRADE–MANHATTAN AREA, GALLATIN COUNTY, MONTANA: SUPERPOSITION GROUNDWATER MODELING REPORT

Mary Sutherland

Montana Bureau of Mines and Geology
Ground Water Investigation Program

MBMG
Montana Bureau of Mines and Geology

Front photo: A scenic ranch in the Gallatin Valley. Photo by Mary Sutherland, MBMG.

HYDROGEOLOGIC INVESTIGATION OF THE BELGRADE–MANHATTAN AREA, GALLATIN COUNTY, MONTANA: SUPERPOSITION GROUNDWATER MODELING REPORT

Mary Sutherland

Montana Bureau of Mines and Geology
Ground Water Investigation Program

Montana Bureau of Mines and Geology Open-File Report 756

2023

Montana Bureau of Mines and Geology

TABLE OF CONTENTS

FIGURES

TABLES

ABSTRACT

Residential and commercial development in and near the communities of Belgrade and Manhattan, in Gallatin County, Montana, have replaced areas of historically agricultural land. Municipal water distribution and wastewater-treatment systems are being installed due to an increasing residential population that often relies on municipal or public water supply. Population estimates for Gallatin County exceed 100,000, with reported growth of 32.9% from 2010 to 2020 (U.S. Census Bureau). Growth is expected to continue, and water availability to supply this growth is a major concern.

The Montana Bureau of Mines and Geology conducted a groundwater investigation in the Belgrade–Manhattan area to better understand groundwater resources. Surface-water flow, stage, and groundwater elevations were monitored and used to develop a groundwater flow model for the area. The model was developed to assess the expected magnitude and location of influence of new pumping stresses within the study area. The model suggests that pumping in thicker deposits of sediment, south of the Central Park fault, offers the least disruption to the flow system. Results also indicate that mitigation of stream depletion via an infiltration pond is effective when applied at a constant rate year-round.

PREFACE

This report has been prepared by the Montana Bureau of Mines and Geology (MBMG) Ground Water Investigation Program (GWIP). The purpose of GWIP is to investigate specific areas, as prioritized by the Ground-Water Assessment Steering Committee (2-15-1523 MCA), where factors such as current and anticipated growth of industry, housing, and commercial activity, or changing irrigation practices, have created elevated concern about groundwater issues. Additional program information and project ranking detail can be accessed at http://www.mbmg.mtech.edu/, Ground Water Investigation Program. GWIP uses various scientific tools to interpret hydrogeologic data and investigate how the groundwater resource has responded to past stresses and to project future responses.

This report summarizes construction of numerical groundwater models and associated results within the context of the study area and the issues addressed. This report is intended for use by qualified individuals, hydrogeologists, and decision-makers to evaluate and use the groundwater flow models or to test specific scenarios of interest, or to provide a starting point for a site-specific analysis. The files needed to run the models are available on the web page for this publication.

INTRODUCTION

The Belgrade–Manhattan study area is in the north-central portion of Gallatin County (fig. 1). It primarily encompasses the floodplains of the Gallatin and East Gallatin Rivers, extending outward into the surrounding foothills. The study area covers about 177 mi^2 of the upper Missouri River watershed (fig. 1). Gallatin County is the fastest growing county in the State (U.S. Census Bureau, 2023), and county planners are concerned about water supply to meet the demand of a growing population. Since 1993 the Upper Missouri River Basin above Morony Dam has been subject to a Legislative Closure, indicating the "DNRC may not process or grant applications for permits to appropriate water or applications for state water reservations within the Upper Missouri River basin" (Water Rights Bureau, 2016). This closure dictates that any new surface-water right must be offset (or "mitigated") by retiring preexisting water rights or proving that existing surface-water flows will not be affected by the new appropriation. Applications to appropriate groundwater for domestic, municipal, and non-consumptive uses are allowed if they do not affect surface-water flows to the Missouri River. Effects can be legally offset by applications to store high spring flows.

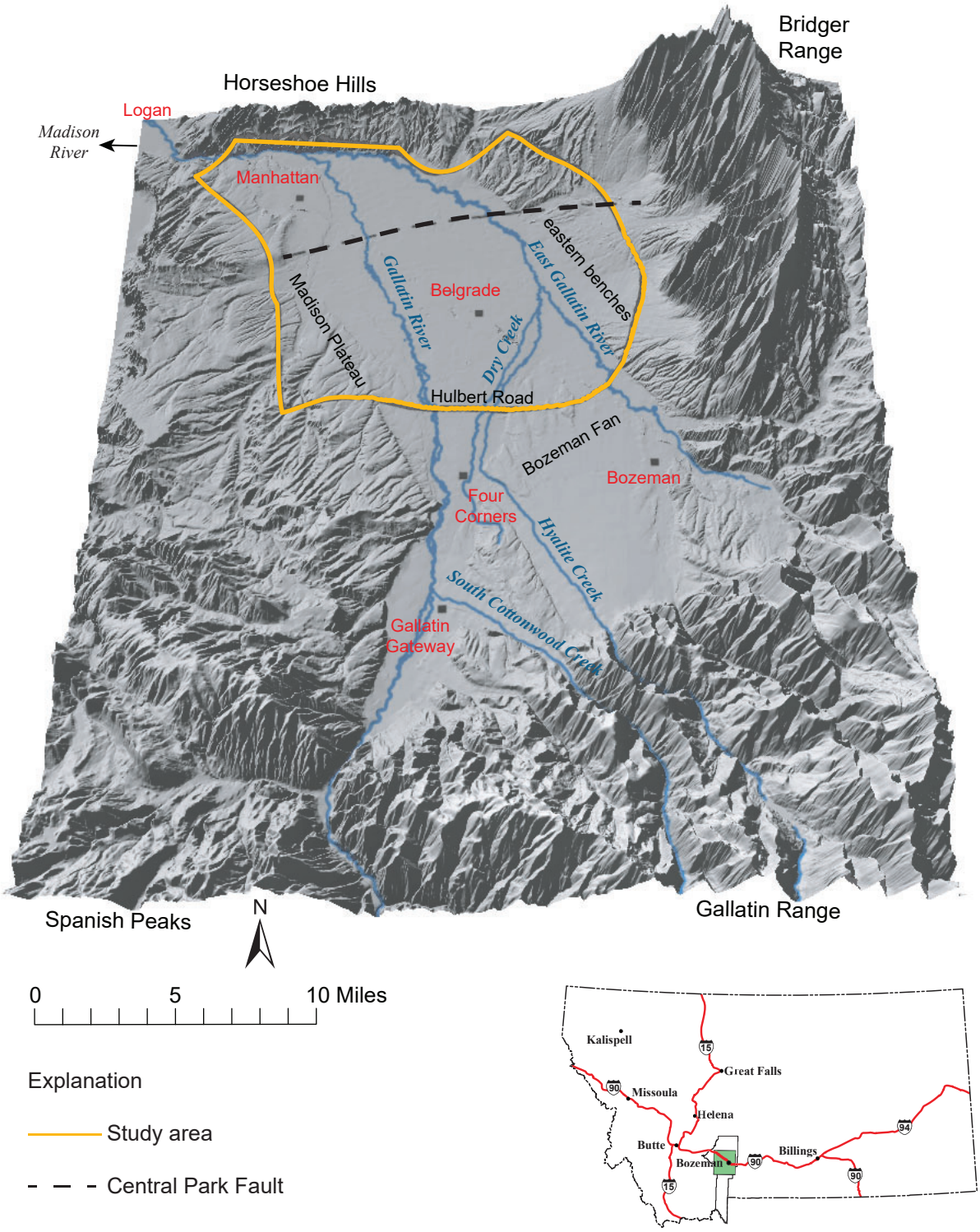

Figure 1. The study area is in Gallatin County, Montana, primarily encompassing the northern portion of the Gallatin River Valley.

Purpose and Scope

This project addresses the following objectives:

1. determine where water is available for public water supply (PWS) use based on hydraulic characteristics of the aquifer, and
2. determine effects on surface water and groundwater from new PWS water use and the feasibility of offsetting those effects.

The location and yield of PWS wells determine the availability of water supplies and the ease of mitigation. This study was conducted to better understand the effects of well placement and mitigation within the Belgrade–Manhattan study area.

Two types of models were used to assess the effects of high-yield pumping on the aquifer and surface waters: an analytical two-dimensional model, and a three-dimensional numerical groundwater flow model. These models will be referred to hereafter as the analytical model and the numerical model.

Municipal and Domestic Water Supplies

The rapid population increase and associated development in the Gallatin Valley necessitates the development of new water supplies. As of 2021, there were 20 active PWS districts that meet residential water demand; many new homes are served by a PWS rather than individual wells. Historically, most suburban development was supplied by individual domestic wells. Figure 2 is a map of the water and sewer districts in the study area, the PWS wells, and other high-yield wells (greater than 500 gpm), typically used for irrigation.

Previous Investigations

Murdoch (1926) conducted the first known study relating groundwater, surface-water, and irrigation effects in the Gallatin Valley. He concluded that groundwater recharge from irrigation, combined with poor drainage in the valley, caused flooding of agricultural land in the north valley.

Hackett and others (1960) provided a comprehensive assessment of hydrologic conditions in the Gallatin Valley. Hackett's report presents geologic mapping, groundwater levels, and streamflow data collected from an extensive monitoring network that was active between 1952 and 1953. The report allows comparison of hydrologic conditions in the early 1950s to conditions described in this study. Hackett and others (1960) concluded that groundwater resources could supplement surface water for irrigation during dry years and be used to expand irrigation to uncultivated acres. By dividing the study into geologic subareas, Hackett and others (1960) also identified the hydrologic and geologic controls on groundwater and surface-water movement throughout the valley.

Dunn (1978) collected groundwater samples and groundwater-level data to evaluate conditions after the Hackett and others (1960) report was completed. Slagle (1995) examined hydrologic conditions in the Gallatin Valley to assess the effects of land-use change. Neither Dunn (1978) nor Slagle (1995) reported notable changes to local water supplies.

Dixon (2002) examined aquifer properties based on drillers' log information and categorized local hydrogeologic units. Custer and Schaffer (2009) and Schaffer (2011) assessed groundwater/surface-water interaction, describing the close connection between the two. These studies provide details of the geology and hydrogeology in the Gallatin Valley.

English (2018) identified areas with greatest potential for developing wells that yield greater than 950 gallons per minute (gpm). Using a framework of 12 "hydrogeologic subareas" identified by Hackett and others (1960), English compiled previously published geologic and hydrogeologic information, aquifer test data, and well log information from the MBMG Ground Water Information Center (GWIC, 2016) to identify these potential high-yield areas. The study area for this GWIP report generally encompasses the Belgrade, Manhattan, and Central Park subareas, first described by Hackett and others (1960) and later modified by English (2018), which is one of the most promising areas for producing sustainable high well yields (fig. 3).

Numerous other, local-scale hydrogeologic studies completed in the Gallatin Valley and the Belgrade–Manhattan area include master's theses and consultant reports submitted for water-rights applications. These materials were reviewed but not specifically cited as a part of this study.

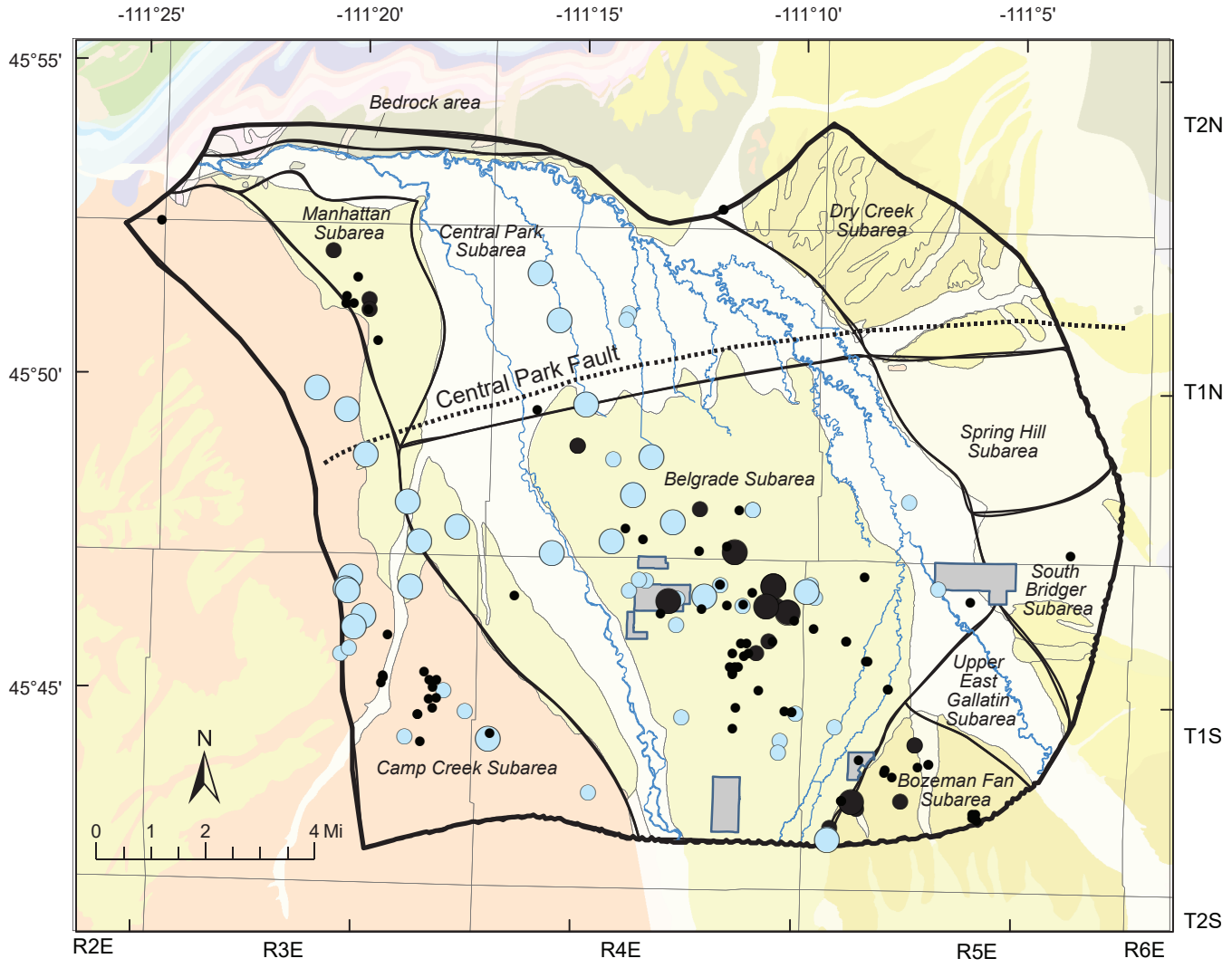

High yield wells

>1000 gpm

- Public water supply
- Other

500-1000 gpm

- Public water supply
- Other

<500 gpm

- Public water supply

Water and Sewer districts

Figure 2. The map shows the locations of public water wells, water and sewer districts, and high-yield wells. The locations of high-yield well may indicate the possibility of locating a public water supply well. As development continues, the area is increasingly dependent on public water supplies.

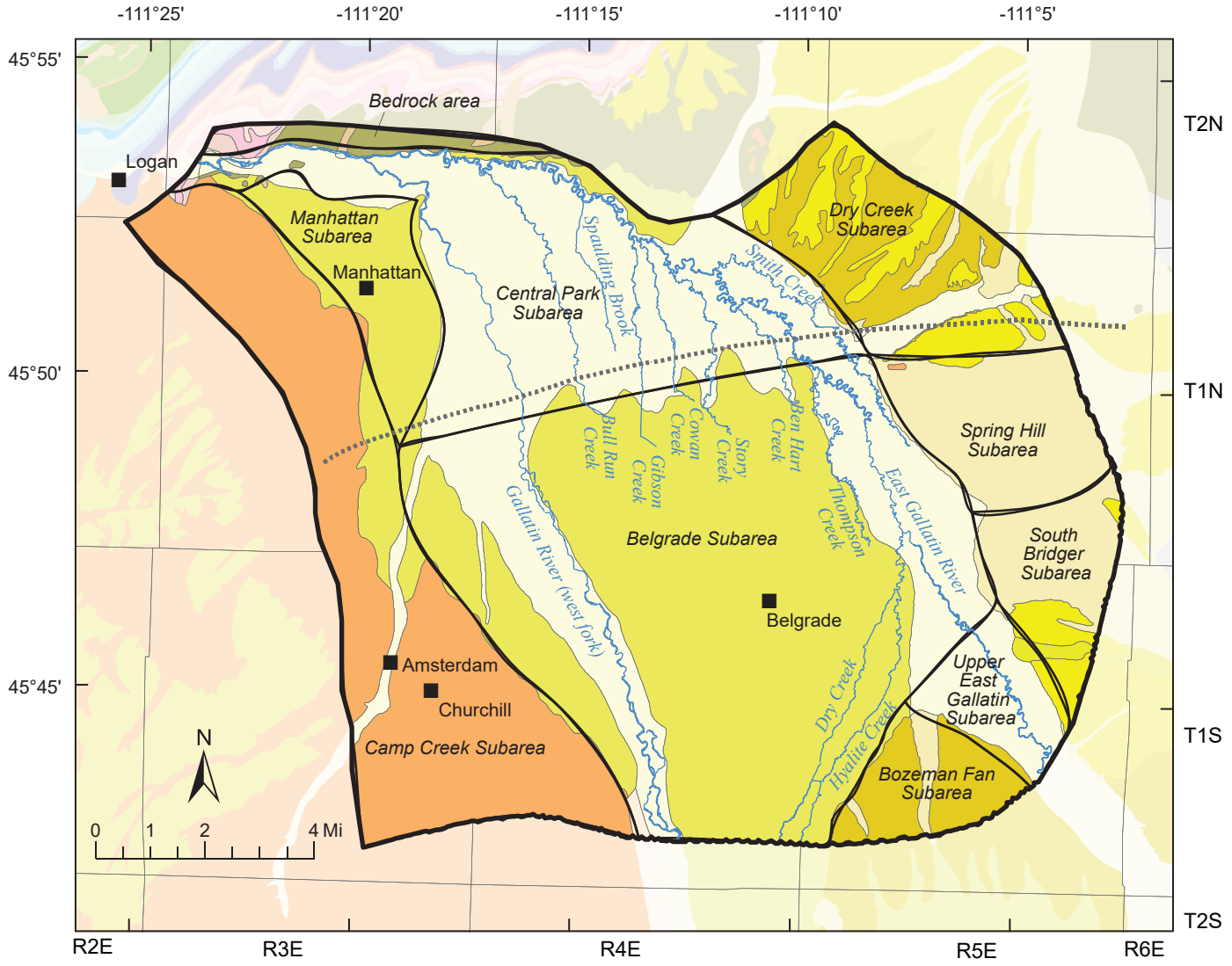

Central Park Fault

Subareas

Geology		Hydrogeologic Units
Qal	Alluvium	Quaternary alluvial sediments
Qat	Alluvial terrace deposits	
Qaf	Alluvial fan deposits	
Qab	Braid plain alluvium	
Qafo	Alluvial fan deposit, older	
QTaf	Alluvial fan deposit	
Tst	Tertiary deposits	Tertiary sediments
€m	Meagher Limestone	Fractured bedrock
€w	Wolsey Shale	
€f	Flathead Formation	
Yla	LaHood Formation, undivided	

Figure 3. The study area is divided into hydrogeologic subareas that reflect sediment deposition and the influence of the Central Park fault's hydraulic control on the aquifer. Subareas are modified from Hackett and others (1960) by English (2018) to reflect the current understanding of the Central Park fault location. Geology is adapted from Vuke and others (2014).

Physiography

The Gallatin Valley covers about 540 mi^2 and occupies the eastern half of the Three Forks structural basin (Robinson, 1961). The valley is bounded by the Horseshoe Hills to the north, the Bridger Range on the east, and the Gallatin Range and the Spanish Peaks of the Madison Range to the south. The Madison Plateau forms the western boundary of the Gallatin Valley (fig. 1), and forms a topographic divide between the Gallatin and Madison River Basins.

The study area consists of a relatively flat valley floor that includes the Gallatin River floodplain and the higher-elevation benches, referred to collectively as the Bozeman Fan area. The area slopes approximately north–northwest following the overall orientation of the Gallatin Valley. Elevations range from 5,210 ft above mean sea level (amsl) on the plateau of the Bozeman Fan to 4,490 ft amsl at the northwestern boundary. Topographically low areas include the streambeds of the Gallatin River, Hyalite Creek, and Dry Creek (fig. 1). The Bozeman Fan area consists of mounded alluvial fan deposits that form hills at the southeastern portion of the study area (Hackett and others, 1960). These sediments rise about 50 to 100 ft above the adjacent floodplain.

The Gallatin River is the primary surface-water feature in the Gallatin Valley. The river flows into the valley from Gallatin Canyon at the southern (upstream) end of the valley near the community of Gallatin Gateway (fig. 1). The Gallatin River flows along the western portion of the study area, and includes tributary waters from South Cottonwood Creek. The Gallatin River's largest tributary, the East Gallatin River, flows along the east side of the study area. The outlet for both surface water and groundwater is a bedrock notch near the town of Logan (fig. 1; Hackett and others, 1960).

Dry Creek and Hyalite Creek are tributaries to the East Gallatin River. These streams flow through the study area and meet the East Gallatin River east of Belgrade. Dry Creek is spring-fed and originates south of the study area. Hyalite Creek flows roughly parallel to Dry Creek, but originates in the Gallatin Range to the south.

Geologic Setting

The geology of the Gallatin Valley was most recently described by Vuke and others (2014; fig. 3). Previous geologic mapping includes Hackett and others (1960), with detailed descriptions provided by Custer and others (1991), Slagle (1995), Dixon and Custer (2002), and Lonn and English (2002). Hackett and others (1960) and Slagle (1995) provide information on the flow regime and hydrogeology of the basin.

The Gallatin Valley is a typical intermontane basin formed by extensional faulting that resulted in gently east-tilted valley floor deposits (Kendy and Tresch, 1996; Vuke and others, 2014). The eastern and southern margins of the valley are defined by several steeply dipping normal faults along the front of the Gallatin and Bridger Ranges.

The valley is divided by an east–west-trending Basin and Range extension fault, the Central Park fault, first described by Hackett and others (1960). The fault is understood to have been active during the deposition of sediments that constitute the study area. South of the fault, a depressed basin was created and is believed to have dropped as much as 4,000 ft. This allowed for the deposition of a thick sediment package in the northern portion of the Belgrade subarea. North of the fault, the offset is described as less than 200 ft, creating a much thinner depositional environment (English, 2018). The fault forms a boundary between the Central Park and Belgrade subareas and transects the Dry Creek and Camp Creek Hills subareas.

Two general groups of sediments were identified in the study area: (1) Quaternary alluvial and Gallatin River floodplain sediments that cover the valley floor; and (2) Tertiary sediments that presumably underlie the entire valley and form benches generally east and west of the modern floodplain (fig. 3). These unconsolidated sediments exchange water and form a single heterogenous aquifer unit (Hackett and others, 1960).

The Quaternary-age sediments are further subdivided into separate formations, based on relative age and provenance (fig. 3, map units Qal, Qat, Qaf, Qab, Qafo, and QTaf). These units are generally cobbles, sand, gravel, and silt/clay deposited by current and recent river channels and alluvial fans or terraces and can be tens to hundreds of feet in aggregate thickness. It is often difficult to separate the Quaternary and upper Tertiary sediments; therefore, the undifferentiated

zone has been included in the Quaternary sediment package, as it is generally found to be more similar in composition to Quaternary sediments at shallow depths.

Underlying the Quaternary sediments are generally finer-grained lower Tertiary sediments (fig. 3, map unit Ts). These materials are characterized by variably cemented sediments, siltstones, sandstones, and conglomerates. Together, these units can be over 1,000 ft thick.

Bedrock underlies the Quaternary and Tertiary sediment, frequently at unknown depths. Very few wells have encountered bedrock within the lower half of the valley, and the only bedrock outcrops within the study area occur north of the Gallatin River in the bedrock area noted in figure 3. North of the Gallatin River, bedrock exposures outcrop in the Horseshoe Hills (fig. 3, map units Ꞓm, Ꞓw, Ꞓf, and Yla).

Hydrogeologic Framework

Surface water and groundwater are connected in the study area (Hackett and others, 1960; Kendy and Tresch, 1996). Groundwater flows west from the eastern benches and Bridger Mountain Range toward the Gallatin Valley floor and north from the Bozeman Fan and Gallatin Mountains parallel to the Gallatin River. The Horseshoe Hills bound the valley to the north, driving water into the gorge between the Madison Plateau and the Horseshoe Hills (fig. 1).

Simplification and grouping of hydraulic characteristics into the subareas defined by Hackett and others (1960) and English (2018) facilitated calibration of the model. In this study, the subareas from Hackett and others (1960) have been modified only to move the boundary created by the Central Park fault and to truncate the areas for the focus of the model.

The Central Park fault, located just north of Belgrade (fig. 3), transects the study area and constrains vertical groundwater flow in the valley. The fault is buried and its precise location is not known. In addition, the fault likely tilts steeply rather than acting as a vertical sediment boundary; evidence from drilling near the fault suggests it has a far-reaching influence on the aquifer between the Central Park and Belgrade subareas. Bedrock on the south side of the fault is several hundred feet lower than on the north side, and consequently contains a much thicker sequence of overlying sediment. The Quaternary/Tertiary alluvial aquifer south of the fault extends to over 1,000 ft in thickness in places, while north of the fault it can be less than 100 ft thick. This rapid shallowing of the aquifer in the dominant flow direction causes groundwater to discharge at the land surface, where it forms several shallow spring-fed creeks (fig. 3). The creeks flow northward and form tributaries to the East Gallatin River. Nearer the confluence of the Gallatin and East Gallatin Rivers, groundwater discharges to marshy areas at the ground surface.

A brief description of the geology of each subarea is included in subsequent sections to provide information about the hydraulic properties of the sediments (table 1). A comprehensive description of the geology can be found in Hackett and others (1960). Reported well yields in each subarea were reviewed for this study (http://mbmggwic.mtech.edu/).

Dry Creek

The Dry Creek subarea is primarily located in the steeply dipping foothills of the Bridger Mountains (fig. 3). Tertiary sediments underlie interspersed, thinly deposited Quaternary alluvial fan deposits (Vuke and others, 2014). There are two existing PWS wells drilled in the alluvial valley at the far eastern corner of the subarea with reported yields of 100 gpm. There are no reported hydraulic conductivities for the aquifer in this subarea; most of these wells are domestic (also referred to as “exempt”) wells completed in the Tertiary sediments with yields less than 100 gpm. Hackett and others (1960) described the subarea as “well drained and contain[ing] little groundwater.” For this reason, the area was not considered suitable for development. In the model, it provides a distal boundary for pumping in the central part of the valley.

Spring Hill

The Spring Hill subarea, also located at the foot of the Bridger Mountains (fig. 3), is almost entirely Quaternary alluvial fan sediments deposited on fine-grained Tertiary sediments. The hydrogeology has not been described, though it is assumed to be similar to the Dry Creek subarea. There are no PWS wells here, nor are there reported hydraulic conductivities in the subarea. Reported well yields are low (<100 gpm). The subarea was included in the model as a distance boundary, but is not considered suitable for high-yield pumping.

Table 1. Aquifer properties of the subareas.

Hydrogeologic Subarea	Data Source	Sediment Age[a]	Transmissivity (T) (ft^2/d)	Hydraulic Conductivity (K) (gft/d)	Storativity (S)
Dry Creek	N/A	—	—	—	—
Spring Hill	Hackett and others (1960)	Q	936–4,010	—	—
South Bridger	Breuninger and Mendes (1993)	Q/T	761–1,700	—	0.00003–0.00017
	Kaczmarek (2003)	Q/T	182–205	—	0.00005–0.00025
	Gaston (1996)	Q/T	254	—	0.00023
	Hay (1997)	Q/T	608	—	0.00066
Upper East Gallatin	N/A	—	—	—	—
Camp Creek Hills	Hackett and others (1960)	T	160–3,476	1–9	—
	Hackett and others (1960)	T	3,476	—	—
Bozeman Fan	Hackett and others (1960)	Q	602–8,689	80	—
	Hackett and others (1960)	T	40–361	—	—
	Custer and others (1991)	Q/T	214–10,694	—	—
Manhattan	Hackett and others (1960)	Q	16,042–18,715	1,043	0.001
	Carstensen (2008)	T	1,955–2,580	21–30[b]	—
Central Park	Hackett and others (1960)	Q	5,080–64,167	201–535	0.006–0.05
	Hackett and others (1960)	T	495	—	0.00001–0.0008
	This study	T	—	26969	—
Belgrade	Hackett and others (1960)	Q	6,684–89,566	602	—
	Hackett and others (1960)	T	2,273	31	—
	Michalek and Sutherland (2020)	Q	—	90–150	0.01–0.001
	Michalek and Sutherland (2020)	T	—	11–73	0.0008–0.00001
	Kendy and Bredehoeft (2006)	Q	1,604–4,679	16–104	—
	Kendy and Bredehoeft (2006)	T	5–307	1–67	—

[a]Q Quaternary; T, Tertiary-age sediments.

[b]K estimated using 1.5 times the screened interval.

South Bridger

The South Bridger subarea is composed of alluvial fan sediments of varying age. The area hosts more wells than the Spring Hill and Dry Creek subareas, but yields are similarly low (≤100 gpm). There is one PWS well with a reported yield of 60 gpm in the area, though most wells are for domestic use. While there are no reported hydraulic conductivities for this area, the estimated transmissivity range is much lower than in other subareas (table 1). Previous studies did not document high yields (English, 2018), suggesting that similar to Spring Hill and Dry Creek, this subarea has low potential for municipal use. The area is included in the model as a distance boundary.

Upper East Gallatin

The Upper East Gallatin subarea differs from those discussed above that border the Bridger foothills in that it is primarily composed of fine-grained Quaternary alluvium deposited by the East Gallatin River (Hackett and others, 1960; English, 2018; Vuke and others, 2014). Alluvial sediments up to 160 ft in thickness have been reported. Tertiary sediments that underlie the alluvium provide a greater yield than com-

parable units to the north; however, the fine-grained nature of the Tertiary sediments limits the yield for municipal use (English, 2018). There are no reported hydraulic conductivities or transmissivities for this subarea. Well yields ranging up to 450 gpm in domestic wells are reported in this area. Although there is currently no existing PWS, the aquifer in the Upper East Gallatin subarea may support low-volume municipal pumping, though it is unlikely to sustain high yields. It is included in the model to provide a distance boundary and baseflow to the East Gallatin River.

Bozeman Fan

The Bozeman Fan subarea is a topographic high on the valley floor composed primarily of outcropping Tertiary basin-fill sediments (Lonn and English, 2002). Compacted, fine-grained sediments, characteristic of Tertiary deposits, likely result in lower well yields than areas with coarser Quaternary sediments; however, there are several reported high-yield wells (>1,000 gpm). Hackett and others (1960) report a transmissivity (T) range of 602 to 8,689 ft^2/d, and Custer and others (1991) reported transmissivities ranging up to 10,694 ft^2/d (table 1). One PWS well reports yields greater than 1,000 gpm, and several others report 400 gpm or greater. Hackett and others (1960) and English (2018) question the sustainability of high-yield pumping in this area due to the limited storage potential of the fine-grained sediments. The high transmissivities reported in this area may be due to productive but laterally discontinuous gravel lenses that may not sustain long-term pumping. The subarea may have potential for relatively low-yield municipal water development, though it was not included in the model as a pumping location.

Camp Creek

The Camp Creek subarea is composed primarily of fine-grained Tertiary sediments above the valley floor on the adjacent Madison Plateau (Vuke, 2003). Although Tertiary sediments are commonly more compacted and/or finer-grained than Quaternary sediment, this subarea has produced multiple high-yield wells. Most are used for irrigation, with reported yields up to 900 gpm. Several PWS wells report yields up to 290 gpm. Hackett and others (1960) reported a T up to approximately 3,476 ft^2/d. The existence of multiple high-yield irrigation wells suggests there may be higher K in some areas (table 1). The high yields are attributed to gravel beds in the sediments (Custer and others, 1991). This subarea was not considered for municipal water development in the numerical model primarily due to the distance from the focus area on the valley floor.

Manhattan

The Manhattan subarea is north of the Central Park fault (fig. 3). Drill cutting indicates that south of the fault, the Quaternary alluvium is highly porous and conductive. North of the fault, these same sediments are characterized by finer-grained sediments with more sand, silt, and clay and typically extend to less than 60 ft in depth. Tertiary sediments reportedly include a deep water-bearing zone from 215 to 300 ft that is partially connected to recharge from infiltration at the land surface (English, 2018). Hackett and others (1960) report a T of up to 18,7115 ft^2/d for the Quaternary, while Carstensen (2008) reports the T of Tertiary sediments to be up to 2,580 ft^2/d (table 1). Several PWS wells are completed in the Tertiary sediments, including wells for the city of Manhattan (500–850 gpm), indicating that the subarea supports high-yield pumping. Irrigation recharge is an important source of water for this area (English, 2018). Pumping wells were not simulated in this subarea because the extent and thickness of Tertiary sediments are not well defined and the shallow alluvium does not appear to support high-yield pumping.

Central Park

The Central Park subarea includes a geologic depositional environment similar to the Manhattan area. Several spring creeks emerge in the subarea or just south of it and are thought to be associated with the thinning of the Quaternary sediments due to the Central Park fault. Groundwater flows to the surface where the offset of deep (~2,000 ft) sediments south of the fault converge with shallow (~500 ft) sediments to the north. Swampy areas and a shallow water table (<15 ft) are characteristic of the subarea near the confluence of the East Gallatin and Gallatin Rivers. Hackett and others (1960) report T in the Quaternary sediments at a range up to 64,167 ft^2/d (table 1). The finer-grained Tertiary sediments are less conducive to high-yield pumping; however, there are four well logs reporting yields over 500 gpm in the Tertiary sediments. One PWS well reports 50 gpm.

Belgrade

The Belgrade subarea is the largest of this study and the most likely to yield high flow rates to wells. Bounded to the north by the Central Park fault, the Belgrade subarea encompasses a thick package (≥2,000 ft) of basin-fill sediments resulting from the downward offset of the fault. Quaternary alluvium in this area is coarse and poorly sorted, with transmissivities reported up to 89,566 ft²/d (table 1; Hackett and others, 1960). The T of Tertiary sediments is on the order of 5–2,273 ft²/d, and there are several PWS wells completed in both Quaternary and Tertiary sediment packages. Reported yields for the PWS wells reach 2,000 gpm and they are drilled up to 450 ft deep.

METHODS

Data Management

Data collected for the Belgrade–Manhattan investigation is stored in MBMG's GWIC database (http://mbmggwic.mtech.edu/). GWIC contains information on well completions, groundwater levels, aquifer tests, and other information. GWIC identification numbers reference locations and sites where data were collected for this report. The data associated with this study are presented under the Belgrade-Manhattan project code on the GWIC website.

Groundwater and Surface-Water Monitoring

Data from 50 wells located within or near the study area were used to examine the subsurface geology of the study area. Existing wells were selected for the monitoring network based on well availability, well owner permission, historical record, geographic location, and hydrogeologic setting. Wells and data from a monitoring network established by the Gallatin Local Water Quality District and the MBMG's Ground-Water Characterization Program were also used. Wells and surface-water sites were monitored generally monthly from the spring of 2012 through 2015. All well logs are available in the MBMG's GWIC database (http://mbmggwic.mtech.edu/, under Belgrade/Manhattan).

Eighteen surface-water monitoring sites were included in the model (fig. 4; appendix A, table A2). Instantaneous field measurements of discharge were obtained using either a Sontek RiverSurveyor Acoustic Doppler Current Profiler, a Sontek FlowTracker Acoustic Doppler Velocimeter, or an OTT MF-Pro electromagnetic current meter. Stage was measured manually at staff gages, from surveyed locations on bridges, and from stilling wells in which dataloggers were installed. Three U.S. Geological Survey (USGS, 1999, 2017a, 2017b) gaging stations also provided historic stage and discharge data for the Gallatin and East Gallatin Rivers (USGS sites 06043500 and 06052500 on the Gallatin and 06048650 on the East Gallatin).

For many streams in the Gallatin Valley it is not possible to measure flows during high flow. During the runoff season (April through June/July), flows are too fast and deep to accurately and safely measure. Additionally, stage data are generally not available during the winter months because of ice buildup at the gage sites. Wells and stream gages used to provide water levels were surveyed by licensed surveyors.

Aquifer Tests

Aquifer tests for this study were conducted at four sites (pumping wells 267822, 255476, 259074, and 266830, fig. 4). Four to six wells were drilled at each location, with monitoring wells arrayed around a production well. Each test consisted of at least 1 week of pre-test water-level monitoring, up to 7 d of pumping, and an appropriate recovery interval. Water levels were measured using pressure transducers (data loggers). Manual water-level measurements were used to correct water levels and ensure that the pressure transducers functioned properly. A digital flow meter and recorder were used, where possible, during testing to record flow rates and the total volume of water pumped.

These tests were conducted and analyzed in accordance with ASTM standards (ASTM, 2008, 2012) to determine the transmissivity, hydraulic conductivity, and storage capacity of the shallow Quaternary aquifer and the underlying Tertiary sediments. The data collected and compiled into a Form 633 during these tests are available in GWIC, searchable with the identification number of the pumped well (fig. 4).

Estimates of aquifer properties are also available from water-rights applications obtained from the Montana Department of Natural Resources and Conservation (DNRC, 2011, 2016) and previous studies. Two aquifer tests performed external to this study, one performed for River Rock Subdivision and one for water right application 41H30029944, were also used

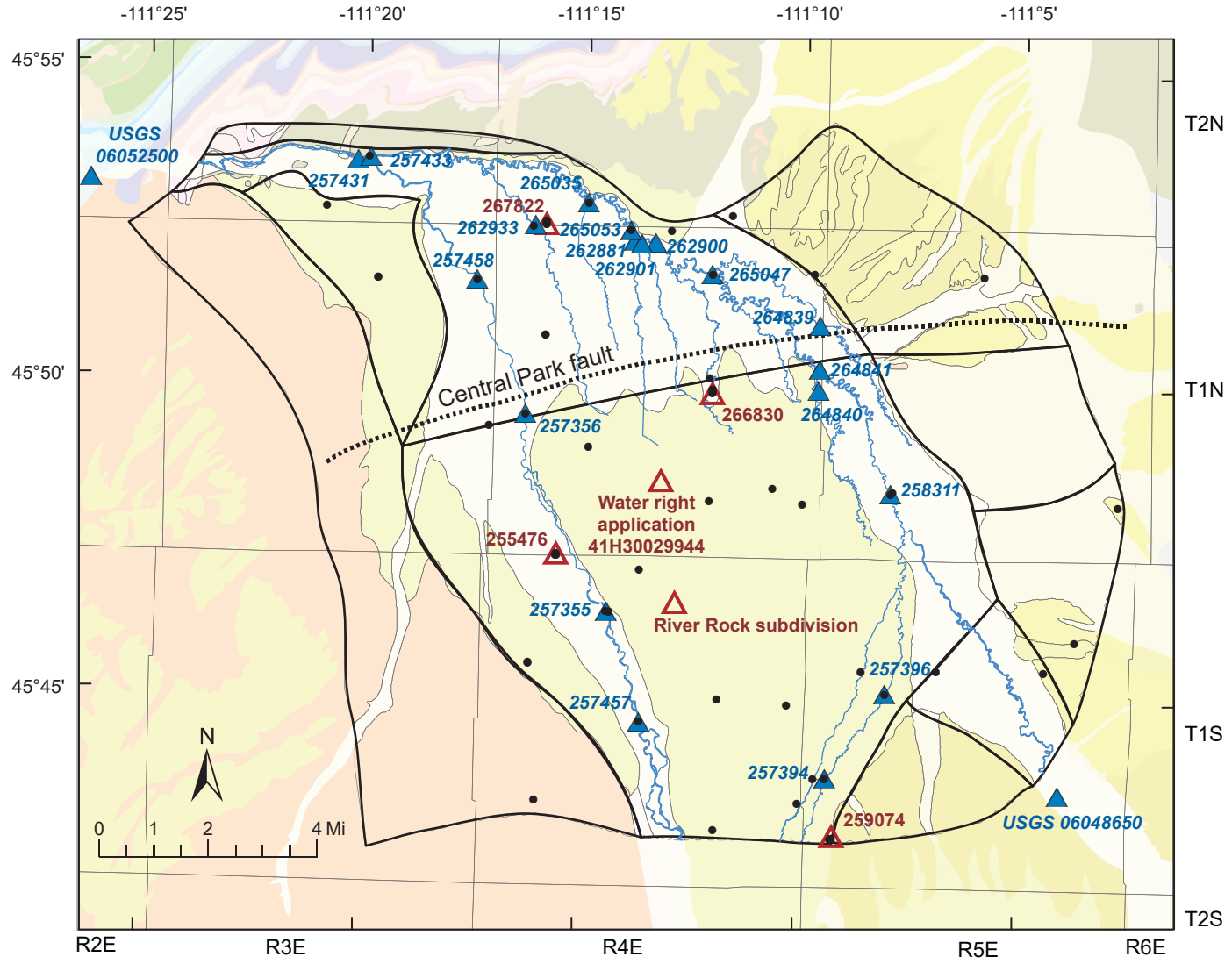

△ Aquifer test sites

▲ Surface-water monitoring sites used to develop the numerical model

• Groundwater monitoring network

Figure 4. Groundwater and surface-water monitoring, drilling, and aquifer testing helped create a conceptual model of the study area that was used to both develop and verify the numerical model. USGS stream gage site 06043500 is south of the study area boundary.

to match pumping conditions in the modeling effort (fig. 4).

Groundwater Modeling

Analytical Model

The analytical model provides a simple approach to analyzing the aquifer system and serves as a preliminary tool to assess aquifer characteristics and effects of pumping. This model incorporates a single well with a constant pumping rate, and estimates the resulting drawdown and/or stream depletion. Assumptions include a homogenous and isotropic aquifer system of infinite lateral extent. This type of model provides a first-cut estimate of the expected drawdown from pumping in various parts of the aquifer and was used to validate the numerical models. The analytical model solves the Theis equation to determine groundwater drawdown at a particular time and distance from the pumping well based on hydraulic characteristics and pumping rates.

The analytical model uses Microsoft Excel 2016 to solve the Theis (1935) distance-drawdown equation

with the Lohman (1979) well function modification to allow for vertical water flow and partially penetrating wells in the aquifer (Lohman 1979; eq. 45, 48). This analytical model allows the user to define storage, transmissivity, time, and discharge to solve the mathematical equation for drawdown at a given distance from the pumping source. The model is limited in function to determining the cone of depression at some distance from a pumping well and acts as a verification tool for the numerical groundwater model (details in appendix A).

The analytical model was developed based on observed and published hydrogeologic properties of the aquifer in the study area. Further assumptions include instant release of water from storage in a non-leaking confined aquifer.

Superposition Numerical Groundwater Flow Model

The numerical model was developed in MODFLOW with steady-state and transient versions to examine four hypothetical pumping scenarios. The MODFLOW model domain encompasses the study area, which extends north from Hulbert Road into the Horseshoe Hills, immediately north of the East Gallatin River to the canyon near Logan. The model extends into the surrounding hills, with the Madison Plateau to the west and the eastern benches acting as a boundary in the foothills of the Bridger Mountain Range (fig. 1).

The purpose of the numerical model is not to predict future conditions or to replicate the current flow regime, but rather to understand the changes that can be expected due to pumping new wells. The superposition model solves the groundwater flow equation in terms of changes to the system rather than in absolute values of head or flow. Rather than calibrating the model to head or stage, estimates of aquifer thickness, conductivity, and transmissivity are used to define the system. The initial model represents current conditions, and each scenario applies a new stress. Changes in groundwater and surface-water conditions are quantified by subtracting the initial model from the scenario model. In this way, the difference in the volume of water by surface-water reach or by aquifer zone can be identified within the overall flow system.

Water use and redistribution of water occur within the model area; however, the principle of superposition holds these factors constant to determine effects on the aquifer. Agricultural recharge, municipal water supply pumping and septic recharge, and evapotranspiration are all considered constant stress factors. Any changes to the system are calculated as an addition or subtraction from the baseline model. If water were to be added to the system, it may induce additional surface-water capture, which is effectively an increase in surface-water flows.

The numerical model employs the principle of superposition to allow for the evaluation of a stress to the system (i.e., pumping of a well) when other stresses to the system are not clearly defined (fig. 5; Bear, 1979). The initial background conditions are constant between the unmodified baseline model and the modified model with a new stress added, negating any effect between the two scenarios other than changes induced by the new stress. By subtracting the second model from the first, all influences aside from the new pumping well are equal, calculating only the changes from the new pumping. For example, a new pumping well might discharge 4 acre-ft/yr of water (Q; fig. 5), and this composite solution indicates 3

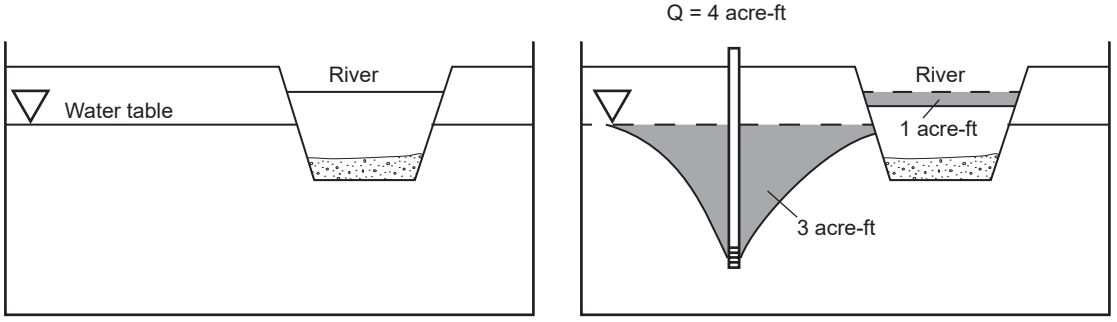

A. Initial flow system

B. Pumping induced drawdown and stream capture

Figure 5. The superposition numerical model allows changes to be subtracted from the initial, baseline flow model (A) to quantify the effects. In this example, the 4 acre-ft of water pumped from the well is from the aquifer (3 acre-ft) and surface-water capture (1 acre-ft).

acre-ft come from storage (aquifer drawdown), and stream depletion (surface-water capture) accounts for the other 1 acre-ft. In this way, the model can compute the expected drawdown and surface-water capture of a new pumping stress without detailed consideration of other background factors.

The superposition model quantifies drawdown and surface-water capture from multiple new stresses with variable pumping rates in a complex hydraulic system. Rather than match the reality of a complex system and calibrate to known water levels or flows, the numerical model mathematically renders the overall characteristics of the system. A superposition model is best used to understand the changes to the system from an applied stress.

Numerical Model

The numerical model uses MODFLOW version 1.19.01, a groundwater flow model developed by the USGS (Harbaugh and others, 2000). The MODFLOW finite-difference equation was solved using the Strongly Implicit Procedure (SIP1) solver (Stone, 1968) and automated parameter estimation (PEST, v. 13.0; Doherty, 2003, 2010). Groundwater Modeling System (GMS version 10.0.2; Aquaveo, 2014) was used as a graphical user interface for MODFLOW and PEST. This software facilitates the use of geographical information such as maps and images for model input and output.

This model simulates groundwater and surface water in the Belgrade–Manhattan area, and the results demonstrate how surface water and groundwater respond to pumping stresses. The model simulates "scenarios" that quantify changes in the hydrologic system that may be useful in making decisions about how and where to locate a municipal water supply well. Each scenario calculates volume and timing of water recharge or discharge by simulating a new stress and comparing the results to the initial (baseline) version. The head changes between the scenario model and the initial model quantify changes in the groundwater system. We use changes in the cell-by-cell flow depletion zones to quantify changes to surface water along any stream reach.

The model represents the basin-fill alluvium of the groundwater system in the study area with five layers. Both the steady-state and transient models are downloadable from the MBMG publications website. These models cover a 177 mi^2 area, and the MODFLOW grid is oriented north–northwest (fig. 6), parallel with the dominant groundwater flow direction.

Steady-State Superposition Numerical Model

Steady-state models are useful for evaluating the overall, long-term effects of changes to the groundwater system and/or average annual characteristics. This steady-state numerical model simulates average annual conditions of the Gallatin Valley for the 2014–2016 water year. Details of the model development are included in appendix A.

The numerical model is based on observed groundwater and surface-water elevations, stream flows, aquifer test results, and previously published data pertinent to the study area. The calibration dataset included monthly stages recorded for surface-water bodies, observed flow data from 2015, and hydraulic characteristics of the aquifer. The calibration reflects the hydrogeologic properties of the subsurface, surface-water flows, and groundwater response to pumping.

Variables that fluctuate throughout the year, such as groundwater elevation, recharge/discharge from canals, and surface-water levels are entered as average values for the year. For example, the elevation of the water surface in the Gallatin River at a site may fluctuate between 4,294 and 4,298 ft over the year; however, the annual average or "steady-state" elevation might fall closer to 4,295 ft. The steady-state model represents the system's response to average annual water conditions.

Transient Superposition Model

The annual changes in recharge, discharge, and flow are broken out by month in the transient model. The transient model is useful for determining the timing of any changes that occur, in both groundwater and surface water, and identifying how different surface-water bodies change over time.

Transient models simulate aquifer system response to time-dependent changes to stresses. For example, a transient model might simulate changes in groundwater levels in response to seasonal pumping. The advantage of the transient model is it can better replicate changes that occur over time. For example, additional water withdrawal from a well may initially cause an increase in groundwater drawdown; however, over

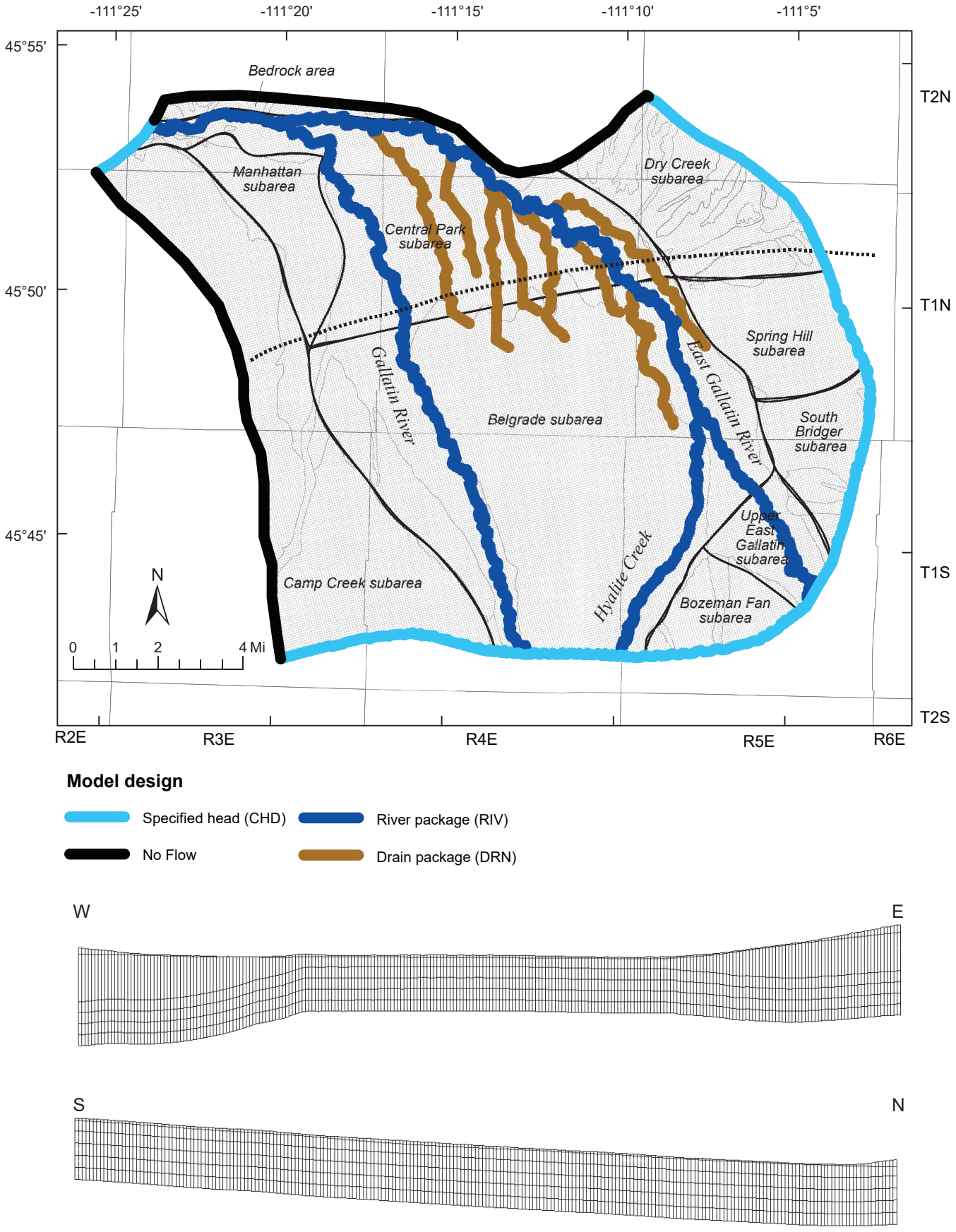

Figure 6. The numerical groundwater model grid is oriented north–northwest to approximate the direction of groundwater flow. The focus of the model is the central part of the valley in the Belgrade, Central Park, and Manhattan subareas. Boundaries are generally located several miles from the focus area, in the hills surrounding the valley. Model details are included in appendix A (table A1). Five layers were used.

time it may include some capture of surface water too. The transient model can quantify the volume of water from each source (e.g., aquifer, streams, rivers) during each stress period.

This transient numerical model builds on the steady-state model to include a time element and includes aquifer storage (S). Fluctuations in monthly surface-water levels and seasonal drainage from irrigation canals to the water table represent flow changes. The transient model evaluated the seasonal response of surface-water changes in Hyalite Creek, East Gallatin, and Gallatin Rivers. Hypothetical pumping scenarios used this model to determine drawdown and changes to surface-water discharge. We present two versions of the transient model. A 12-mo transient model simulates January 1, 2015 through January 1, 2016. A 10-yr transient model replicates the conditions of the 12-mo version through December 31, 2025. The 10-yr transient model provides a baseline, or control model, for comparison to new stresses applied in the predictive scenarios.

Model Construction

The subareas are a modification of Hackett's (1960) subareas based on areas of geologic deposition (fig. 3). Simplification and grouping of the hydraulic characteristics into these subareas streamlined the calibration of the model.

The geologic units were consolidated into three main hydrogeologic units for the purpose of estimating K in the model: bedrock (Ꞓm, Ꞓw, Ꞓf, Yla), Tertiary sediments (Tsuf, Tsuc, Tdc), and Quaternary sediments (Qal, Qat, Qaf, Qab, Qafo, QTaf; fig. 3). The Quaternary/Tertiary contact is often difficult to distinguish in drill cuttings and only clearly identifiable at the surface. In addition, Quaternary sediments interfinger with the Tertiary sediments in some locations, causing mixing or interbedding of the deposits. For these reasons, the Quaternary and Tertiary sediments, unless identified at the surface or clearly identified in drill cuttings, were grouped into hydraulic conductivity zones.

The bedrock of the valley floor is generally outside of the interest of this study, and its hydraulic characteristics are poorly characterized. It is primarily comprised of limestones, shales, and sandstones with low porosity as compared to the unconsolidated deposits (Vuke and others, 2014). The bedrock is frequently weathered to saprolite near the surface, and is commonly fractured. Water movement in the bedrock is dominantly through saprolite and fractures.

Tertiary sediments tend to be less transmissive than the Quaternary deposits, owing to a greater proportion of fine sediments. The Tertiary sediments are characterized by matrix-supported siltstones and sandstones, calcareous cemented zones, and conglomerates. These sediments include some lenses of silt and clay, cemented layers, and compacted layers. The composition is similar to Quaternary sediments, though the Tertiary sediments tend to have a higher limestone component (Vuke and others, 2014).

Quaternary sediments in the valley are the youngest and generally the coarsest, with higher K. They are composed of alluvial fan, terrace, and braided river deposits of the valley floor. The sediments are characterized by moderate to well-sorted sands and gravels with sparse clay or silt layers. The composition varies but is primarily clast-supported bedrock of quartz, quartzite, volcanics, and Archean metamorphic rocks (Vuke and others, 2014).

Monthly average stage data for the East Gallatin near Bozeman (USGS station 06048650) and the Gallatin River near Logan (USGS station 06052500) were applied to the inflow of the East Gallatin River and the outflow of the Gallatin River. All other stage data from Belgrade–Manhattan project locations were applied to nodes corresponding to GWIC locations.

The stage values were duplicated annually to develop a 10-yr baseline numerical model for comparison to the pumping scenarios. No new stresses were applied in the 10-yr numerical model, which runs from January 1, 2015 to January 1, 2026. The time steps were decreased from 5 to 1 for each month to make the numerical model run more efficiently.

RESULTS

Numerical Model

The model includes five layers and divides the domain into nine subareas to distinguish geologic characteristics governing groundwater movement. The depth, rather than the age, of the sediments dictate hydraulic conductivity in the Belgrade, Manhattan, and Central Park subareas. The sediments are similar in composition; however, they typically fine and com-

pact with depth. The hydraulic conductivity decreases with depth in the model to account for this. Horizontal K (HK) was modeled by subarea, depth, and geologic source material by determining a minimum and maximum range within each model layer and subarea. Shallow alluvial deposits were assigned the highest K while consolidated Tertiary deposits and bedrock were assigned the lowest K.

The fluvial and alluvial sediments are composed primarily of the same source material; however, stratification of the fluvial deposits inhibits vertical movement of water. In areas of shallow fluvial sediments (Upper East Gallatin, Belgrade, Manhattan, and Central Park areas), the vertical conductivity (VK) is limited to approximately 10% of HK (table 2). In deeper sediments where water movement is limited by compaction or in areas of alluvial deposits, vertical conductivity is approximately 33% of HK (Alan English, MBMG, oral commun., 2019). We applied these ratios as anisotropy factors to VK within the Layer Properties Flow package of MODFLOW.

Fractured bedrock occurs at shallow depths north of the Gallatin River and in the Dry Creek, Spring Hill, and South Bridger subareas, but otherwise occurs at depths below this model domain. In the Dry Creek Subarea, model layers 3–5 simulate bedrock, and in a small section north of the river, all five model layers represent bedrock.

The low-K bedrock is included in the calculation of conductivity for all subareas except Belgrade, where the depth to bedrock exceeds 500 ft. Bedrock exposures at the far north part of the study were included in layer 1 (figs. 7–9).

Tertiary sediments were included in the calculation of hydraulic conductivity for all subareas, though they are thinner in the Dry Creek, Spring Hill, and South Bridger areas (figs. 7–9). Where Quaternary sediments are exposed at the surface, they were included in the calculation of HK for the subarea (fig. 9).

Tertiary fine sediments are at shallow depths north of the fault, ranging from 20 to 80 ft below ground surface (figs. 7–9). Layer 1 north of the fault is similar in composition to the valley fill of the Belgrade subarea, but deeper geologic material has lower HK. Similar Tertiary sediments are present south of the Central Park fault (fig. 9) at depths ranging from 200 to 400 ft, with compaction causing lower HK at greater depth (fig. 9).

Sediments in the Belgrade subarea are heterogenous, with lateral and vertical variation in hydraulic conductivity. Coarse Quaternary and shallow Tertiary sediments fill the valley bottom from the southern end, deepening as the valley tilts toward the fault. Highly conductive sediments occur at depths of 200 ft or more in the central part of the valley. These sediments fine and compact with depth, decreasing HK, but are more productive than sediments north of the fault. Surficial Tertiary sediments in the Bozeman Fan subarea have a lower HK than surrounding valley sediments, and the coarse alluvium of the Upper East Gallatin subarea overlies shallow Tertiary sediments from the same fan deposition. The upper 200 ft of the valley floor subareas south of the fault generally has the highest conductivity.

Dry Creek, Spring Hill, South Bridger, and Camp Creek subareas are included in the model, though they are not the focus of this study. These areas provide a buffer around the area of interest that negates the effects of boundary conditions along the edges of the model. Limited information is available on the hydraulic characteristics of aquifer material in these subareas, and they were estimated during model calibration.

Source and Sinks

Hyalite Creek, the East Gallatin River, and the Gallatin River were simulated using the MODFLOW river package (RIV; fig. 6). This package incorporates observed stage for each river reach over the period of record. The river package calculates gains and losses to the river reach based on streambed conductance and the relationship between stream stage and head in the aquifer. Field measurements of stage and river bottom elevation are entered into GMS nodes (appendix A, table A2). Locations of river reaches were digitized from the 2015 National Agricultural Imagery Program (NAIP, 2015) aerial imagery.

Streambed conductance (C) was calculated for each river reach. The thickness (b) of the streambed was set to 1 ft. The range of streambed permeability for similar streams was taken from Calver, 2005 (see appendix A, table A3 for details). Width was applied at the stream nodes, at locations where the stage and flow were measured in the field. Conductance values were adjusted during model calibration.

Table 2. Modeled aquifer properties.

	Geologic Area	HK Min (ft/d)	HK Max (ft/d)	VK Min (ft/d)	VK Max (ft/d)	Vertical Anisotropy
Layer 1	South Bridger Subarea	1	50	8	26	0.33
	Upper East Gallatin Subarea	10	400	21	205	0.1
	Spring Hill Subarea	5	50	9	28	0.33
	Bozeman Subarea	1	120	20	61	0.33
	Dry Creek Subarea	10	40	8	25	0.33
	Belgrade low Q	10	450	23	230	0.1
	Belgrade high Q	10	600	31	305	0.1
	Bedrock area	1	50	1	25	0.5
	Central Park Subarea	100	350	23	225	0.1
	Camp Creek subarea	1	200	33	101	0.33
	Belgrade low Q	10	450	23	230	0.1
	Manhattan Subarea	15	400	21	208	0.1
Layer 2	South Bridger Subarea	1	50	8	26	0.33
	Upper East Gallatin Subarea	10	30	2	20	0.1
	Spring Hill Subarea	5	50	9	28	0.33
	Bozeman Subarea	1	100	17	51	0.33
	Belgrade	50	450	25	250	0.1
	Belgrade Subarea	10	350	18	180	0.1
	Central Park Subarea	40	200	12	120	0.1
	Manhattan Subarea	10	200	11	105	0.1
	Bedrock area	1	40	1	20	0.5
	Dry Creek Subarea	5	25	5	15	0.33
	Belgrade low Q	10	350	18	180	0.1
	Belgrade low Q	10	350	18	180	0.1
	Camp Creek subarea	1	150	25	76	0.33
Layer 3	South Bridger Subarea	1	45	8	23	0.33
	Upper East Gallatin Subarea	10	30	2	20	0.33
	Spring Hill Subarea	2	50	9	26	0.33
	Bozeman Subarea	1	100	17	51	0.33
	Dry Creek Subarea	1	50	8	26	0.33
	Central Park Subarea	10	75	4	43	0.33
	Camp Creek subarea	1	120	20	61	0.33
	Belgrade Subarea	10	250	13	130	0.1
	Belgrade Subarea	10	300	16	155	0.1
	Manhattan Subarea	10	50	3	30	0.33
	Bedrock area	1	45	1	23	0.5
Layer 4	South Bridger Subarea	1	40	7	21	0.33
	Upper East Gallatin Subarea	10	30	2	20	0.33
	Spring Hill Subarea	2	35	6	19	0.33
	Bozeman Subarea	1	80	13	41	0.33
	Dry Creek Subarea	1	50	8	26	0.5
	Central Park Subarea	10	75	4	43	0.33
	Camp Creek subarea	1	125	21	63	0.33
	Bedrock area	1	20	1	10	0.5
	Belgrade Subarea	10	175	9	93	0.1
	Belgrade Subarea	10	225	12	118	0.1
	Manhattan Subarea	10	50	3	30	0.33
Layer 5	South Bridger Subarea	1	35	6	18	0.33
	Upper East Gallatin Subarea	10	30	2	20	0.33
	Spring Hill Subarea	2	35	6	19	0.33
	Bozeman Subarea	1	75	13	38	0.33
	Dry Creek Subarea	1	50	8	26	0.5
	Belgrade Subarea	1	150	8	76	0.33
	Manhattan Subarea	10	50	3	30	0.33
	Bedrock area	1	20	1	10	0.5
	Central Park Subarea	10	75	4	43	0.33
	Camp Creek subarea	1	125	21	63	0.33

Note. HK, horizontal hydraulic conductivity; VK, vertical hydraulic conductivity; Vertical Anisotropy, ratio of horizonal to vertical movement.

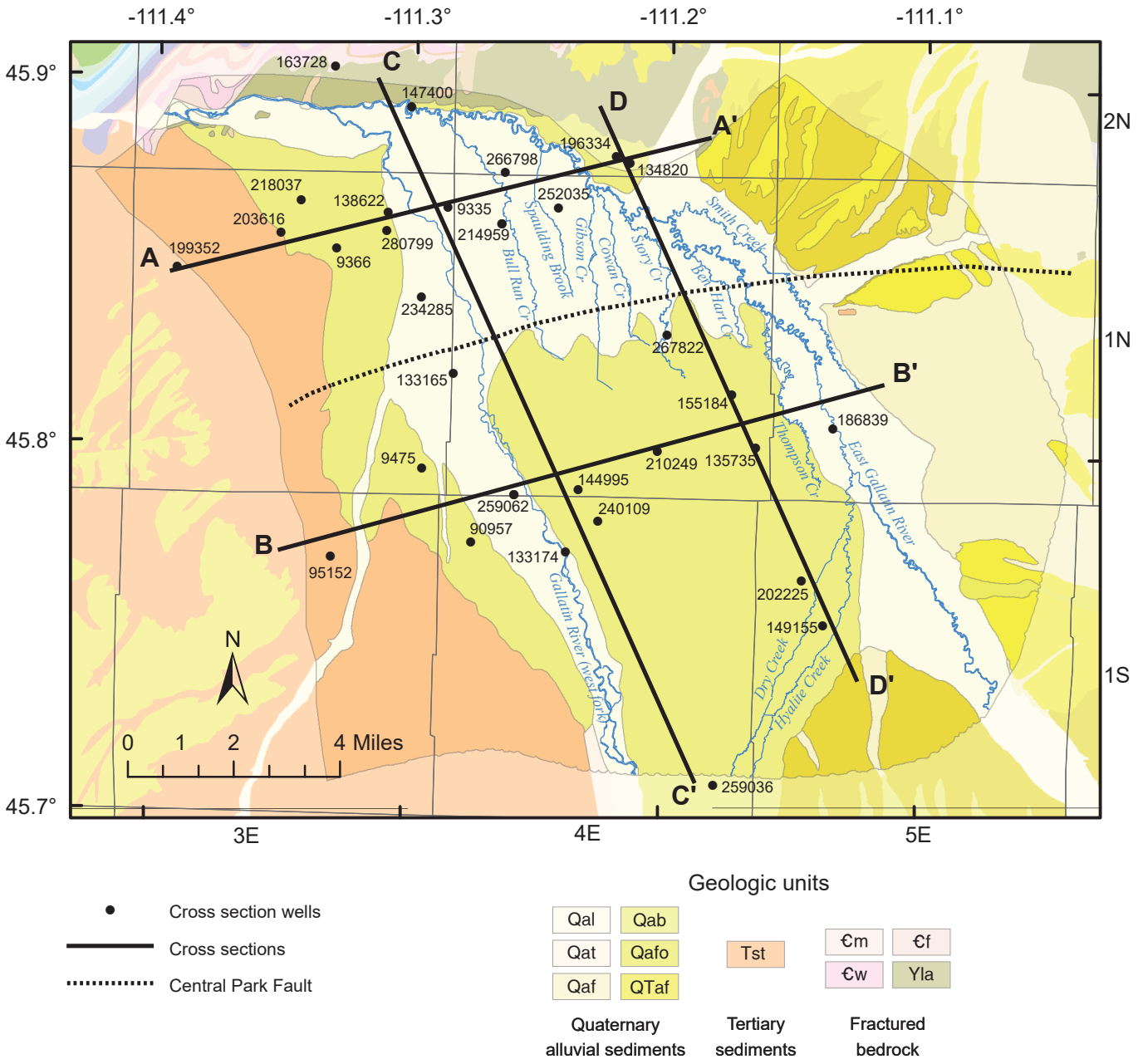

Figure 7. Four cross-sections were developed to better understand the hydraulic conductivity of sediments at depth in the valley. Well logs and geologic maps were examined to determine the depth of the lithology and the hydraulic controls exerted on the aquifer. See figure 9 for lithologic descriptions.

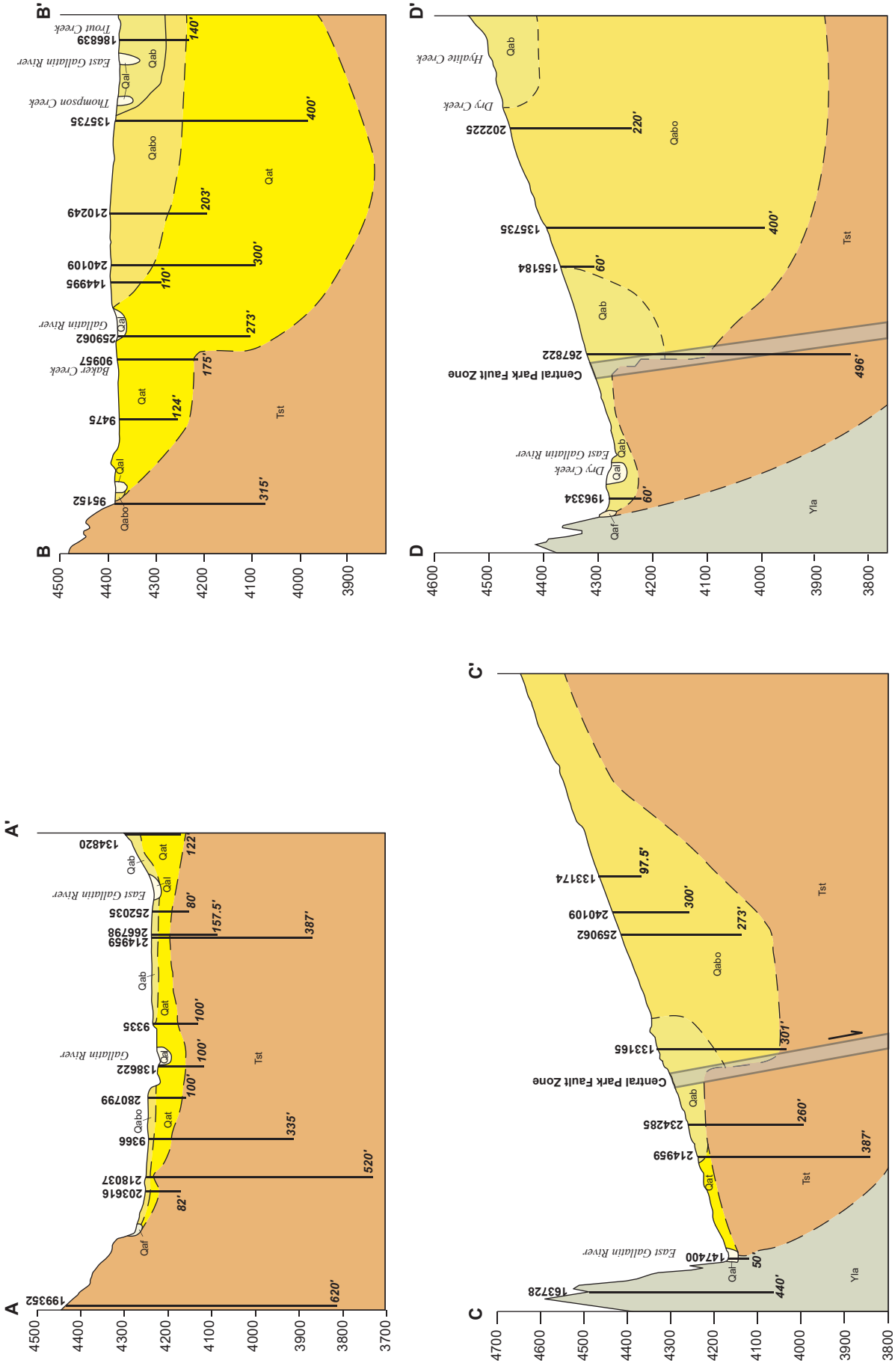

Figure 8. Four cross-sections show the control of the Central Park fault on the depositional environment. Dark lines show wells, with the number at land surface being the GWIC ID number, and the number at the bottom showing total depth. North of the fault (A) Quaternary sediments are significantly thinner than south of the fault (B). Cross-section lines C and D show the Central Park fault dropped to the south, causing a thick package of basin-fill sediments.

Unit	HGU	Description	Modeled area	Thickness where present
Qal	Quaternary alluvial sediments	Alluvium comprised of unconsolidated gravel, sand, silt, and clay in stream and river channels	Central Park, Belgrade, Upper East Gallatin, and Dry Creek subareas	<50 ft
Qat		Alluvial terrace deposits	Dry Creek and Belgrade subareas	Unknown
Qaf		Alluvial fan deposits comprised of gravel, sand and silt deposited by Hyalite Creek	Dry Creek, Spring Hill, South Bridger, and Bozeman subareas	<200 ft
Qab		Alluvial braid plain deposits comprised of bouldery gravel and sand with thin beds of clayey silt	Belgrade and Manhattan subareas	<800 ft
Qafo		Alluvial fan deposits comprised of gravel, sand, silt and minor amounts of clay	South Bridger subarea	<100 ft
QTaf		Alluvial fan deposits comprised of gravel, sand, and silt	Dry Creek and South Bridger subareas	<120 ft
Tsuf	Tertiary sediments	Dominantly fine-grained siltstone with conglomerate sandstone beds and lenses of gravel	Camp Creek (surface), Manhattan, Central Park, Belgrade, and Upper East Gallatin subareas (subsurface)	<300 ft
Tsuc		Dominantly coarse-grained conglomerate with sandstone, siltstone, and volcanic ash beds	Bozeman, Dry Creek (subsurface), and South Bridger (subsurface)	500+ ft
Tdc		Siltstone and fine-grained sandstone with conglomerates and calcareous paleosols	Central Park area (subsurface)	800–1000 ft
€m	Fractured bedrock	Limestone and dolomite	Bedrock area	330–550 ft
€w		Shale	Bedrock area	<400 ft
€f		Sandstone, quartzite, and cemented conglomerate	Bedrock area	<150 ft
Yla		Limestone and shale	Bedrock area (surface), Dry Creek, Spring Hill, South Bridger, Central Park, and Manhattan	Unknown

Figure 9. The geologic controls on groundwater were classified into three main hydraulic groups: the Quaternary alluvium, the Tertiary sediments, and the fractured bedrock. The hydraulic properties of each group, based on aquifer test results, were used as calibration criteria in the numerical groundwater model.

Spaulding Brook, Gibson, Cowan, Story, Ben Hart, Bull Run, lower Smith, and Thompson Creeks were simulated using the MODFLOW drain package. The drain package is similar to the river package; however, the drain package simulates only flow from the aquifer to the drain at nodes where the head in the aquifer exceeds the elevation of the drain. The package does not simulate stream loss (flow from the drain to the aquifer). Elevations at the drain nodes were calculated from digital elevation models where they were not surveyed for the project (see appendix A, table A4 for details).

Each of the streams modeled as drains acts as a sink for groundwater, exclusively simulating the discharge of groundwater to surface water. Limited flow information on the creeks collected during this study demonstrated a hydraulic connection to the aquifer. As coarse geologic materials thin north of the fault, groundwater discharge to springs form the headwaters of these creeks.

Numerical Model Calibration

The goal of a superposition model is to replicate the characteristics of an aquifer and determine the effects of an applied stress; therefore, the steady-state characteristics of the aquifer were targeted rather than trying to match head change. Groundwater elevations collected for the Belgrade–Manhattan study were included as qualitative calibration criteria. The calibration criteria included matching drawdown recorded during three aquifer tests and varying hydraulic conductivity within the measured ranges for each subarea. The model results were compared to the analytical model, the drawdown from three aquifer tests, and the surface-water gains and losses to determine when the calibration was satisfactory (details in appendix A).

Groundwater/Surface-Water Interactions

The gains to or losses from the aquifer along each river reach are simulated as gain to the aquifer (positive flow) or loss from the aquifer (negative flow) between nodes. For example, if the surface-water flow from one node to the next decreases, flow to the aquifer is positive. In GMS, cells of the river arc may gain or lose water individually between nodes, with flow calculated as the sum of the cells constituting the river arc.

In reality, throughout the year, river reaches may change seasonally from gaining to losing, and this makes the steady-state model a simplification. During calibration, flows were maintained within the range of gains and losses from one node to the next. The streambed permeability was modified so that the conductivity term replicated gains and losses. Flow measurements taken on Bull Run, Cowen, Gibson, Smith, and Thompson Creeks near their confluences with the East Gallatin River were input to the model to establish flow. We used flow measurements from 18 locations along these reaches to determine the range of gains along the drain cells. Each creek is modeled as a single arc with an overall negative flow between the point of origin and the terminus at the East Gallatin River.

The simulated flows fall within the range of observed flows for each river segment. Changes in flow are highly variable, particularly in Hyalite Creek where the stream is dam-controlled, and the upper reaches of the East Gallatin River adjacent to the Eastern Benches. Table 3 shows the minimum and maximum measured flows along each modeled arc of the river. Unmeasured diversions or tributaries introduce error to the calculation of gain or loss; this error may account for the wide range in measured flows along some river arcs.

Hydraulic Conductivity

The hydraulic conductivity array was developed using a combination of polygon and pilot point PEST calibration tools. The hydraulic conductivity was adjusted during calibration within measured field conditions in the subareas. An array of pilot points within the subareas allowed a minimum and maximum horizontal hydraulic conductivity, and the array of HK is calibrated to the reported range of values for the geology of the area (fig. 10; table 1). Each layer is heterogeneous, reflecting the variety of geologic units present. Table 2 presents the horizontal hydraulic conductivity assigned to layers 1–5 along with the anisotropy factor applied to generate VK.

The layer one K values are representative of coarse-grained Quaternary sediments in the Belgrade, Manhattan, and Central Park subareas in the shallow sediments crossing the Central Park fault (figs. 3, 10). Horizontal conductivity is lower where layer one includes the finer-grained sediments of the Camp

Table 3. Measured surface-water flows.

GWIC ID or USGS Station No.	Location	Model Arc	Minimum Flow Measured (cfs)	Minimum Flow Measured (ft^3/d)	Maximum Flow Measured (cfs)	Maximum Flow Measured (ft^3/d)	Average Discharge (ft^3/d)	Flow Range (ft^3/d)	Error %	No. of Flow Measurements
6048650	E. Gallatin–USGS gage near Bozeman	EG1	19	1,658,880	446	38,534,400	20,096,640	36,875,520	23.2	Continuous
258311	E. Gallatin–Penwell Bridge	EG2	18	1,516,320	778	67,250,304	34,383,312	65,733,984	44.4	13
264841	E. Gallatin–Dry Creek Rd.	EG4	73	6,324,480	312	26,969,760	16,647,120	20,645,280	4.3	6
265047	E. Gallatin Swamp Rd.	EG5	136	11,759,904	391	33,792,768	22,776,336	22,032,864	2.9	5
262900	E. Gallatin–Dry Crk School Rd.	EG6	149	12,888,288	361	31,152,384	22,020,336	18,264,096	2.4	6
265053	E. Gallatin, W. Dry Crk Rd.	EG7	181	15,616,800	374	32,343,840	23,980,320	16,727,040	2.1	6
265035	E. Gallatin–Spaulding Bridge	EG8	152	13,165,632	418	36,142,848	24,654,240	22,977,216	2.7	5
257433	E. Gallatin–Gallatin River Ranch	EG9	181	15,652,224	576	49,743,072	32,697,648	34,090,848	3.2	14
257431	Gallatin River–Nixon Gulch	GR	284	24,579,936	2,253	194,689,440	109,634,688	170,109,504	7.9	12
6052500	Gallatin River–USGS gage at Logan		223	19,267,200	2,980	257,472,000	138,369,600	238,204,800	13.4	Continuous
N/A	Gallatin–Inflow	WG1		25,937,280		228,556,512	127,246,896	202,619,232	8.8	—
257457	Gallatin–Cameron Bridge	WG2	151	13,080,960	2,366	204,379,200	108,730,080	191,298,240	15.6	11
257355	Gallatin–Amsterdam Rd.	WG3	77	6,626,016	2,073	179,114,976	92,870,496	172,488,960	27.0	11
N/A	Gallatin –STRD	WG5	287	24,788,160	331	28,624,320	26,706,240	3,836,160	1.2	—
257356	Gallatin–Frontage Rd.	WG6	86	7,471,008	303	26,145,504	16,808,256	18,674,496	3.5	10
257458	Gallatin–Dry Creek Rd.		72	6,222,528	1,922	166,101,408	86,161,968	159,878,880	26.7	12
257400	Hyalite Creek–Inflow	HY1		527,040		11,956,896	6,241,968	11,429,856	22.7	1
257394	Hyalite Creek–Valley Center Rd.	HY2	1	55,296	133	11,520,576	5,787,936	11,465,280	208.3	12
257396	Hyalite Creek–Frontage Rd.	HY3	0	37,152	35	2,992,896	1,515,024	2,955,744	80.6	15
264840	Thompson Crk–Dry Creek Rd.	Thompson Creek	14	1,226,880	47	4,043,520	2,635,200	2,816,640	3.3	2
264839	Reese Creek –Dry Creek Rd.	Reese Creek	19	1,610,496	51	4,406,400	3,008,448	2,795,904	2.7	7
262881	Gibson–Dry Crk School Rd.	Gibson Creek	4	362,880	10	889,920	626,400	527,040	2.5	8
262901	Cowen–Dry Crk School Rd.	Cowen Creek	2	211,680	8	709,344	460,512	497,664	3.4	8
262933	Bull Run Cr.–Sales Rd.	Bull Run Creek	1	92,448	9	760,320	426,384	667,872	8.2	10

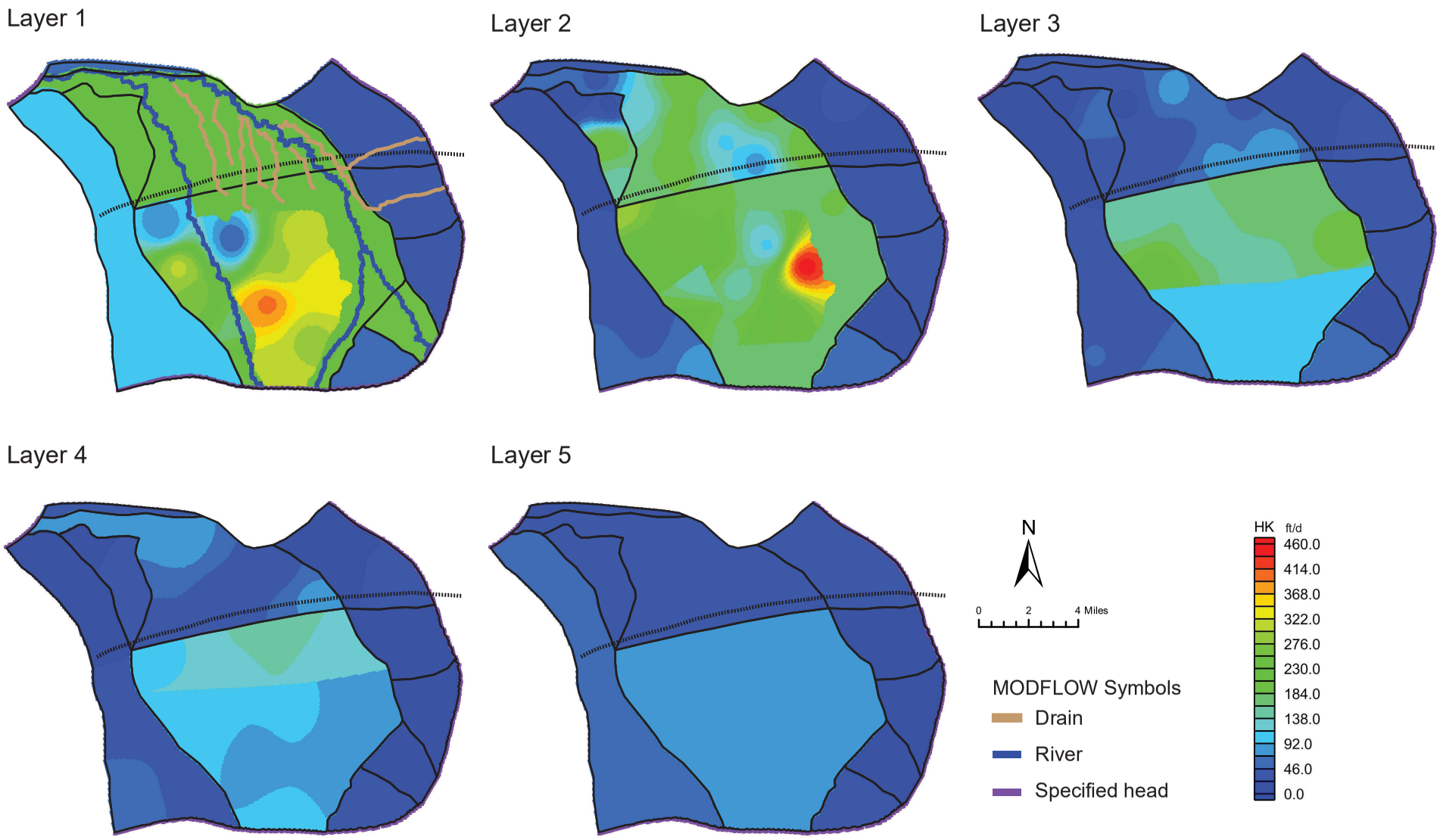

Figure 10. The modeled hydraulic conductivity shows the influence of the sediments on groundwater flow. With the exception of a portion of the Belgrade subarea that includes a thick package of coarse Quaternary sediments, the finer Tertiary sediments decrease hydraulic conductivity as depths increase.

Creek Hills, and lower still in the Tertiary outcropping of the Bozeman Fan subarea. Layer one in the Upper East Gallatin subarea has relatively high K values to represent the shallow fluvial sediments deposited by the East Gallatin River, and K values decrease in the eastern benches of the Dry Creek, Spring Hill, and South Bridger subareas. In the Belgrade subarea, the PEST calibration arrived at high- and low-conductivity areas that are not consistent with our conceptual model of the aquifer system. These areas calibrated poorly; however, changes to the K values negatively affected river flows in the Gallatin River. As such, these high- and low-K areas were retained and used in the scenarios to determine the effects of high- and low-conductivity sediments on the drawdown from pumping.

Layer two has relatively low K values north of the fault, where fine Tertiary sediments are prevalent (fig. 10). Conductivity further decreases near the model boundary that simulates groundwater outflow from the model domain, where bedrock becomes shallow and compacted Tertiary sediments dominate. The relatively high conductivity of the Central Park and southern Manhattan subareas suggest interconnected gravel deposits in the shallow basin-fill sediments. A high-conductivity zone near Belgrade may overestimate the actual aquifer conductivity; however, it occurs in the location of a known deep sediment zone that displays promising aquifer development potential. The hydraulic conductivity decreases near the southern portion of the Belgrade subarea, where coarse Quaternary sediments thin and finer Tertiary sediments dominate. The shallow sediments of the Upper East Gallatin subarea (represented in layer one) are replaced by deeper sediments similar to those in the adjacent subareas in the foothills of the Bridger Mountains. In these subareas (Dry Creek, Spring Hill, and South Bridger), bedrock may be present at this depth or in layers two or three; the low conductivity at depth reflects the low porosity of fractured bedrock.

Model layer three reflects a decrease in conductivity due to an increased percentage of fine sediment and compaction north of the fault (fig. 10). The Belgrade subarea sediments also show decreasing conductivity with depth, although the deep Quaternary package remains an overall relatively high-conductivity zone. The coarsest part of the aquifer has the highest conductivity, reflective of the thick basin-fill sediments encountered on the down-dropped side of the Central Park fault. The Camp Creek Hills, Upper East Gallatin, Manhattan, Central Park, and Bozeman Fan subareas reflect the finer-grained, compacted or cemented Tertiary sediments found at depth in these areas.

Model layer four shows the effect of compaction and increasing cementation from Tertiary sediments both above and below the fault (fig. 10). Wells that exceed 400 ft in depth in the Belgrade subarea encounter the Quaternary/Tertiary boundary, though it is sometimes difficult to distinguish the contact. Tertiary sediments tend to be finer and often include lenses of calcareous or cemented lenses and worm casts that help determine the contact. The sediments reflect compaction and tend to fine with depth, though in the northeast part of the valley there is a coarse sediment package that increases conductivity. Other subareas are composed entirely of finer Tertiary sediments or bedrock at this depth. The modeled conductivity reproduces our conceptual model of the conductivity in these deeper basin sediments.

Model layer five reflects a uniformity of conductivity between the deeper Belgrade subarea sediments and the adjacent Camp Creek Hills subarea, which are both composed entirely of Tertiary sediments (fig. 10). Interconnected gravel beds within the Camp Creek Hills provide zones of productive, high-conductivity aquifer. It is possible that similar beds exist in the deep sediments west of the river. Just as the Camp Creek Hills subarea provides ample water, it is likely that there are conductive zones within the deep basin of the Belgrade subarea; however, the overall conductivity of the Belgrade subarea is likely to be low. At these depths, the only locations that have good water development potential are in the Camp Creek Hills and the Belgrade subareas.

Storage

The 12-mo transient model incorporated aquifer storage and changes over time into the calibrated steady-state model, and simulates January 1, 2015 through January 1, 2016. Storage values for layers one through four were assigned a value of 10%, which represents an unconfined aquifer consisting of sands and gravels (Driscoll, 1986). Layer five was assigned a confined storage value of 0.5% to represent compacted to cemented Tertiary silts and clays.

Numerical Model Verification

Aquifer test data provided calibration targets to match to the output from the transient model. Three 72-h aquifer tests were reproduced in the transient 1-yr numerical model to determine whether the model accurately simulated the observed drawdown. These aquifer tests were part of a water-rights application near Belgrade, water-rights application 41H 30029944 for River Rock subdivision on Amsterdam Road, and a test performed by GWIP on Stagecoach Trail (well 255476). Two other aquifer tests at Sales Road (well 266830) and Hulbert Road (well 259074), performed for this study, were also reproduced but not utilized during calibration. The locations of the tests are shown in figure 4.

The model simulated drawdown similar to the tested wells, including drawdown at nearby observation wells (where available). The results are described in detail in appendix A. By simulating the aquifer tests in the numerical model and obtaining similar drawdown results, the model demonstrates that the match to the calibration targets was sufficient with storage parameters of 10% for layers 1–4 and 0.5% for layer 5.

Model Predictive Scenarios

Predictive scenarios illustrate the potential effects of hypothetical stresses. In this study, the steady-state, 1-yr transient, and 10-yr transient numerical models provide base cases and new stresses are applied to them. Using superposition, we compare the calculated stream depletion and head from applying new pumping stresses to the baseline model. In the predictive scenarios, a pumping rate of 5,000 acre-ft/yr (3,100 gpm) is simulated, either from one well or from an array of wells. The pumping is distributed throughout the year based on estimated domestic consumptive use in the Gallatin Valley (DNRC, 2011). A base rate of 2,007 gpm (270 acre-ft/mo) is pumped from November to April, and pumping increases from May to July as residential irrigation increases water use. A decrease in pumping is simulated from August to October until it reaches the base rates (table 4).

The MODFLOW model simulates the groundwater system, and rather than tracking the volume of surface-water flow, it tracks the gain or loss of groundwater to/from surface water. The model quantifies the volume of groundwater that discharges to surface water at streams and rivers. Groundwater that discharges to surface water is "lost" from groundwater but sustains flow to springs, streams, and rivers. Groundwater discharge to streams and rivers is referred to in these scenarios as "surface-water capture." When surface-water capture declines, this indicates a decrease in the surface-water flow. Changes in water are expressed as positive (groundwater gain) and negative (groundwater loss) quantities. Decreases in surface-water flow

Table 4. Monthly pumping rates for simulated pumping wells.

Stress Period	1 well		81 wells[a]	
January	32,254.6 ft^3	270 acre-ft	398.2 ft^3	3.3 acre-ft
February	32,254.6 ft^3	270 acre-ft	398.2 ft^3	3.3 acre-ft
March	32,254.6 ft^3	270 acre-ft	398.2 ft^3	3.3 acre-ft
April	32,254.6 ft^3	270 acre-ft	398.2 ft^3	3.3 acre-ft
May	48,381.9 ft^3	405 acre-ft	597.3 ft^3	5.0 acre-ft
June	80,636.5 ft^3	676 acre-ft	995.5 ft^3	8.3 acre-ft
July	96,763.8 ft^3	811 acre-ft	1,194.6 ft^3	10.0 acre-ft
August	80,636.5 ft^3	676 acre-ft	995.5 ft^3	8.3 acre-ft
September	56,445.5 ft^3	473 acre-ft	696.9 ft^3	5.8 acre-ft
October	40,318.2 ft^3	338 acre-ft	497.8 ft^3	4.2 acre-ft
November	32,254.6 ft^3	270 acre-ft	398.2 ft^3	3.3 acre-ft
December	32,254.6 ft^3	270 acre-ft	398.2 ft^3	3.3 acre-ft
Annual Total	596,710 ft^3	5,000 acre-ft	596,711 ft^3	5,000 acre-ft

[a]Volume is per well.

indicate a decrease in groundwater discharge to surface water compared to the baseline scenarios.

The simulations include:

3. One well vs. many wells: comparison of the groundwater-elevation changes and streamflow losses induced by pumping a set volume of water from one well compared to pumping the same volume from a group of wells in the same vicinity.

4. Effects of hydraulic conductivity: a comparison of pumping the same volume of water in coarse, highly conductive sediments versus finer-grained, low-conductivity sediments. This includes a comparison of aquifer thickness.

5. Pumping mitigation: in a closed basin such as the Gallatin Valley, any new water rights require legal mitigation by offsetting water use. In this simulation, mitigation is simulated by infiltrating the amount of water pumped at a pond (mitigation wells) in the model.

6. Timing and location of surface-water loss: pumping wells can cause pumping-induced stream losses, depending on the locations of the wells relative to the stream. This scenario compares effects of pumping on various river reaches and examines the timing and volume of stream loss.

The locations of the pumping and/or mitigation wells are shown in figure 11 and the design of the scenarios is shown in table 5.

Scenario 1: One Well vs. Many Wells

The steady-state and transient models were used to evaluate the groundwater and surface-water response to pumping a theoretical PWS well installed in the Belgrade subarea. The theoretical PWS well produces 5,000 acre-ft/yr (3,100 gpm), either as a single well or as an 81-well field pumping the same 5,000 acre-ft/yr from a dense array of wells (fig. 11, inset; BE4 pumping well array). The 5,000 acre-ft/yr is not a constant rate but varies throughout the year (table 4). The single well is in the central part of the valley with the 81-well array surrounding it (fig. 11). Each well in the well field is completed in layer one or two of the model, simulating a depth of 80 ft, and cumulatively the 81 wells are pumping the same volume as the single well (table 5). The single pumping well (BE4; fig. 11) is completed in layer three of the model, at a depth of 300 ft, to accommodate the greater drawdown expected from a single well.

The steady-state model results show that pumping a single well causes a steep cone of depression near the well, whereas pumping 81 wells develops a diffuse cone of depression near the well field. At a mile from the center of the pumping, the cones of depression from these simulations are indistinguishable (fig. 12). Comparison of the pumping-induced surface-water capture from the rivers and streams was nearly identical between the two numerical models. Results show that the number of wells used to pump an equal volume of groundwater does not affect the amount of reduction in discharge to surface water, nor does it change the distribution of drawdown outside of the immediate pumping area (table 6). In the steady-state numerical model, the system has equilibrated to the continuous new stress. In these two simulations, the wells pump 5,000 acre-ft/yr in perpetuity and eventually nearly all water is from a reduction in discharge to surface water rather than from storage. The percent of water pumped that is from a reduction in discharge to surface water is 94% in both steady-state simulations.

The same two scenarios were run in the 10-yr transient numerical model. Figure 13 shows river (13A) and stream (13B) leakage changes superimposed over the baseline scenario with no pumping. Differences in pumping-induced losses from the streams and rivers between the two pumping scenarios were initially different but become similar over time. Pumping initially pulls more water from the rivers, but over time, the surface-water loss shifts to pull more water from streams, although the river loss is a larger volume (figs. 13A, 13B). Pumping-induced surface-water capture by the rivers nears equilibrium, with negligible differences between the two pumping simulations (fig. 13A). The volume of pumped water that would have been discharged to the streams in the baseline model slowly increases, with greater streamflow losses due to pumping from the 81-well field. This difference may be due to the shallow (80 ft) well array having a more direct connection to surface water than the single deep well (300 ft). Groundwater stored in the aquifer fluctuates as pumping rates change. The magnitude of surface-water capture and storage withdrawal reflects increasing and decreasing pumping rates throughout the year. The comparison between the two simula-

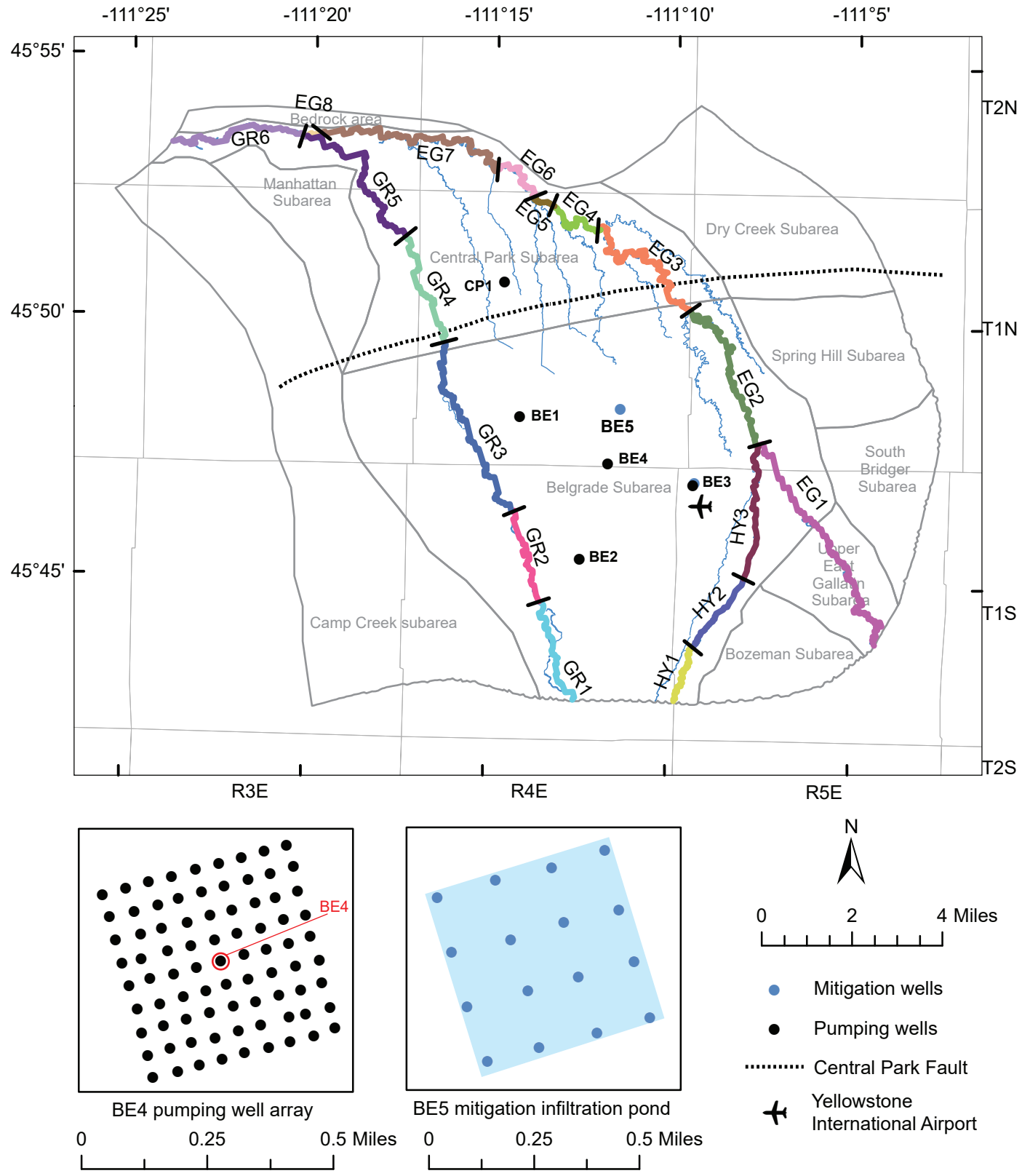

Figure 11. The numerical model breaks the rivers into reaches to assign flow, streambed conductance, and elevations. The predictive scenarios include multiple pumping wells and a mitigation area to allow for new pumping stresses applied to the model.

Table 5. Predictive model scenario designs.

Scenario 1	Description			
Steady-state	Compares a single well pumping to an 81-well array in the same hydraulic conductivity zone			
Well	No. of wells	Well depth	Pumping rate	HK zone
BE4 (pumping)	1	300	5,000 AF-y	300 ft/d
BE4 (pumping)	81	80	5,000 AF-y	300 ft/d
Transient 10-yr	Compares a single well pumping to an 81-well array in the same hydraulic conductivity zone			
Well	No. of wells	Well depth	Pumping rate	HK zone
BE4 (pumping)	1	300 ft	5,000 AF-y	300 ft/d
BE4 (pumping)	81	80 ft	5,000 AF-y	300 ft/d
Scenario 2	Description			
Steady-state	Compares a single pumping well in low HK sediments to a single pumping well in high HK sediments			
Well	No. of wells	Well depth	Pumping rate	HK zone
BE1 (pumping)	1	80 ft	5,000 AF-y	20-50 ft^3/d
BE2 (pumping)	1	80 ft	5,000 AF-y	400-450 ft^3/d
Transient 10-yr	Compares a single pumping well in shallow sediments to a single pumping well in deeper sediments with similar HK			
Well	No. of wells	Well depth	Pumping rate	HK zone
CP1 (pumping)	1	80 ft	5,000 AF-y	200-250 ft^3/d
BE4 (pumping)	1	80 ft	5,000 AF-y	200-250 ft^3/d
Scenario 3	Description			
Transient 10-yr	Compares mitigation through an array of injection wells uniformly throughout the year vs. only in Apr, May, and June			
Well	No. of wells	Well depth	Pumping rate	HK zone
BE3 (pumping)	1	80 ft	5,000 AF-y	300-350 ft^3/d
BE5 (injection/mitigation)	16	5 ft	5,000 AF-y	250-300 ft^3/d
Scenario 4	Description			
Transient 10-yr	Compares the timing and location of surface-water capture from shallow alluvium vs. deeper sediments			
Well	No. of wells	Well depth	Pumping rate	HK zone
CP1	1	80 ft	5,000 AF-y	200-250 ft^3/d
BE3	1	80 ft	5,000 AF-y	300-350 ft^3/d

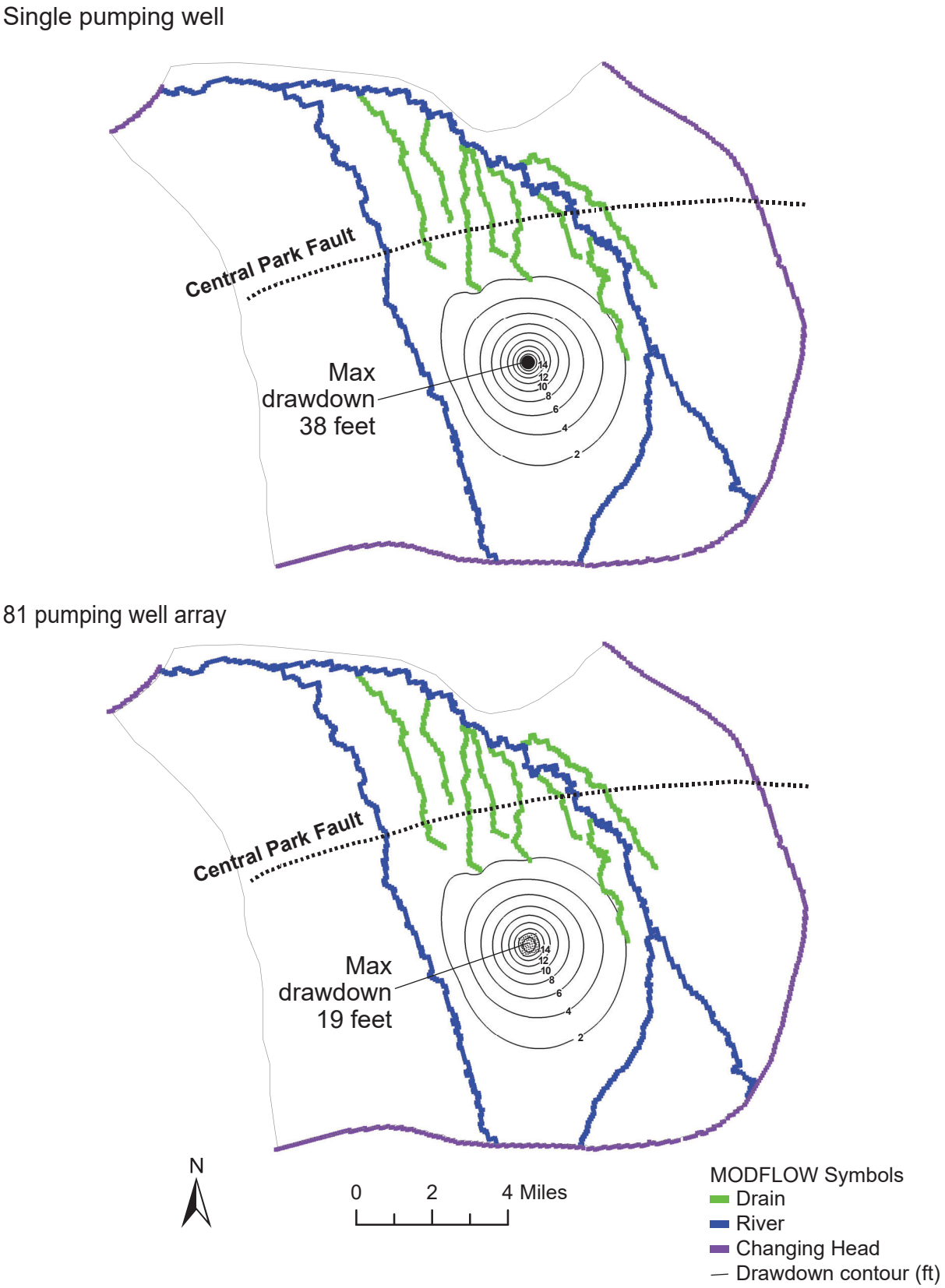

Figure 12. The single pumping well and the 81 pumping well array reflect virtually identical drawdown contours at approximately 1 mi from the pumping center (near the 14-ft contour interval). The drawdown from the single pumping well at the center reaches a maximum of 38 ft while the well array reaches only 18 ft of drawdown.

Table 6. Scenario 1 results for the steady-state model.

Simulation	Stress Applied	River Gain[a] (ft^3)	Stream Gain[1] (ft^3)	Max. Head Drawdown (ft)	Percent Surface Water Sourced for Pumping
Baseline	No pumping simulation	16,044,068	14,156,542	0	0
Scenario 1	BE5 1 well simulation	947,218	824,146	38	94
Scenario 1	BE5 81 wells simulation	947,439	823,760	19	94

[a]Decreases from the "no pumping" scenario indicate decrease in groundwater going to surface water.

tions in this scenario indicates that the volume of water pumped determines the amount of surface-water capture rather than the number of wells that water is pumped from.

Scenario 2: Effects of Different Hydraulic Conductivity Zones on Pumping

The steady-state and 10-yr transient numerical models were used to test the effects of hydraulic conductivity on pumping rates, groundwater drawdown, and pumping-induced surface-water capture. In one simulation, the effects of high and low conductivity were compared, and in another simulation, the effects of similar conductivities with differing thicknesses were compared (table 7).

Using the steady-state numerical model, two pumping wells simulating a PWS producing 5,000 acre-ft/yr were placed in the numerical model in a high-conductivity zone (400–450 ft/d) and a low-conductivity zone (20–50 ft/d). The pumping rates varied throughout the year in the transient simulations (see table 5). The wells are both completed in layer 1 and are located approximately 6,300 ft from the Gallatin River, at locations BE1 (low-conductivity zone) and BE2 (high-conductivity zone; fig. 11). These zones were identified through model calibration and represent the range of HK within the Belgrade subarea (table 1).

In the steady-state numerical model, the low-conductivity pumping well (BE1) induced a head drawdown of approximately 34 ft. The well in the high-conductivity area (BE2) created a drawdown of over 48 ft (fig. 14). Surface-water losses were not equivalent between these two wells, primarily due to the distance from the creeks. While the two wells are equidistant from the Gallatin River, well BE1 is located further north, closer to the creeks that discharge into the Gallatin River (fig. 14). Reduction in groundwater discharge to the creeks, modeled as drain leakage, was nearly three times higher at this location. The

Table 7. Scenario 2 steady-state results.

Simulation	Stress Applied	Depth of Well (ft)	HK Zone (ft/d)	River Gain[a] (ft^3)	Stream Gain (ft^3)	Max. Head Drawdown (ft)	Percent Surface Water Sourced for Pumping
Baseline	None			16,044,068	14,156,542	0	0
Steady-state BE1	One PWS pumping 5,000 acre-ft/yr in low HK zone	80	20–50	841,392	778,546	33.8	95
Steady-state BE2	One PWS pumping 5,000 acre-ft/yr high HK zone	80	400–450	1,038,943	267,836	47.5	96
Steady-state BE4	One PWS pumping 5,000 acre-ft/yr south of fault (thick sediment package)	80	200–250	399,334	2,233,610	40.2	91
Steady-state CP1	One PWS pumping 5,000 acre-ft/yr north of fault (thin sediment package)	80	200—250	832,227	1,505,857	56.3	92

[a]Decreases from the "no pumping" simulation indicate decrease in groundwater going to surface water.

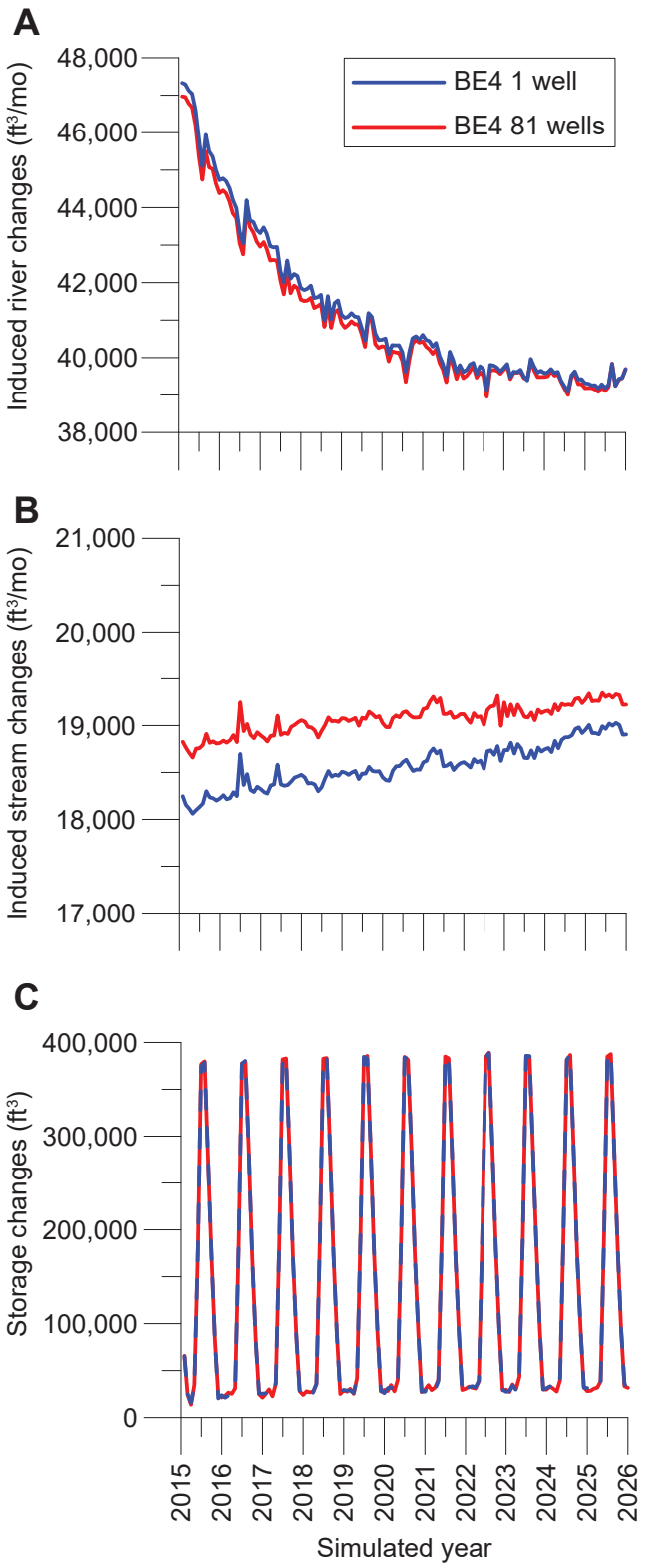

Figure 13. Graphs A and B illustrate the changes in river (A) and stream (B) loss from pumping 1 well or 81 wells as compared to the baseline model with no pumping. The East Gallatin and Gallatin Rivers are responsible for about 4% of the volume pumped, but the losses taper over time (A). Stream capture (B) increases over time, with the 81 well field resulting in a greater volume loss (300–400 ft³/mo) compared to pumping from one well. Storage changes in the aquifer are virtually identical in both pumping scenarios (C).

groundwater discharge to the creeks likely decreased the pumping-induced river leakage, causing river leakage to be lower for well BE1 (table 7). The capture of water at well BE1 that reduced discharge to streams was nearly equal to the capture of water at well BE2 that reduced discharge to the river, with a difference of less than 1% of surface-water capture between the two locations. This suggests that nearly the same volume of water will be captured; however, the source of surface water (stream or river) depends on the location of the pumping well relative to each surface-water body.

A similar steady-state simulation compared two layer 1 wells north and south of the Central Park fault. Well BE4 is south of the fault, completed in the thicker Quaternary sediments (>300 ft) of the Belgrade subarea (HK 200–250 ft/d). Well CP1 is located north of the fault in sediments that have similar hydraulic conductivity (200–250 ft/d) to the location of well BE4 in the shallow surficial sediments (<80 ft). The high-conductivity sediments north of the fault are not as thick, and therefore of lower transmissivity, before reaching the low-conductivity zone of finer Tertiary sediments. The sediments in layer 2 north of the fault limit water availability and deepen the cone of depression. Pumping from either well reduces groundwater discharge to surface water, with the cone of depression extending outward to the spring creeks and both the East Gallatin and Gallatin Rivers.

The same two wells, BE4 and CP1, are simulated in the transient 10-yr numerical model. Pumping from well BE4 captured more groundwater that otherwise would have discharged to surface water when compared to pumping from CP1 (fig. 15A), and it used less water from storage (fig. 15C). This results from proximity to the spring creeks as well as the shallow Tertiary sediments. The increase in drawdown and capture by streams is offset by a greater depletion of the rivers (fig. 15B). The 10-yr numerical model indicates well BE4 captures almost five times as much water that would otherwise discharge to the river than well CP1 when both pumping well scenarios reach equilibrium. Pumping from Well CP1 also causes a greater change in storage from the baseline numerical model as pumping increases and decreases throughout the year (fig. 15C).

As pumping increases throughout the summer months (table 4), the proportion of pumped groundwater intercepted prior to discharge to the river decreases

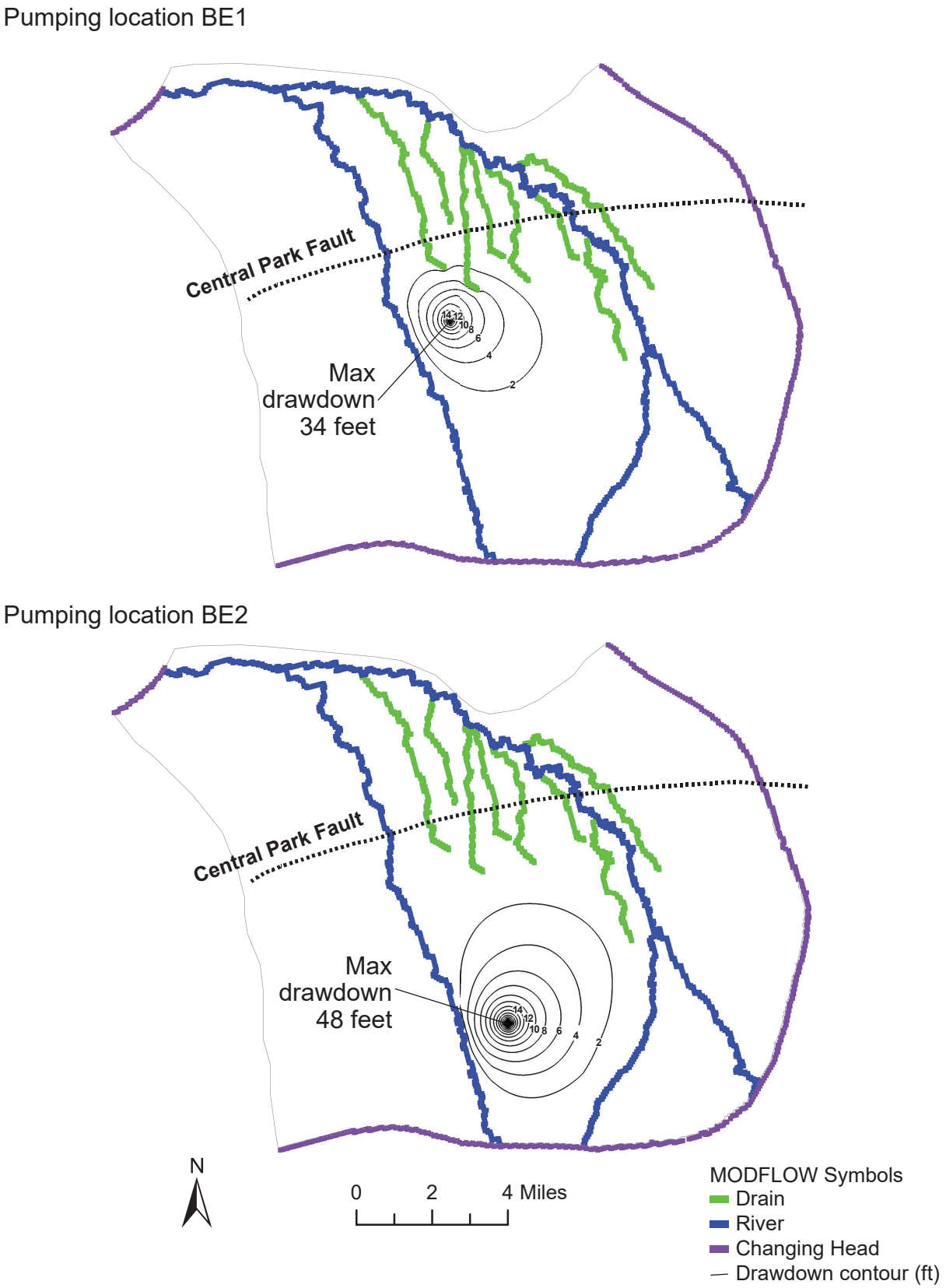

Figure 14. Well BE1 (A) is pumping from a high-conductivity zone (400–450 ft/d) and well BE2 (B) is pumping from a low-conductivity zone (20–50 ft/d). Well BE1 has a narrow cone of depression and a steeper drawdown, while well BE2 has a wider, shallower drawdown. Both wells are pumping 5,000 acre-ft/yr at a depth of 80 ft.

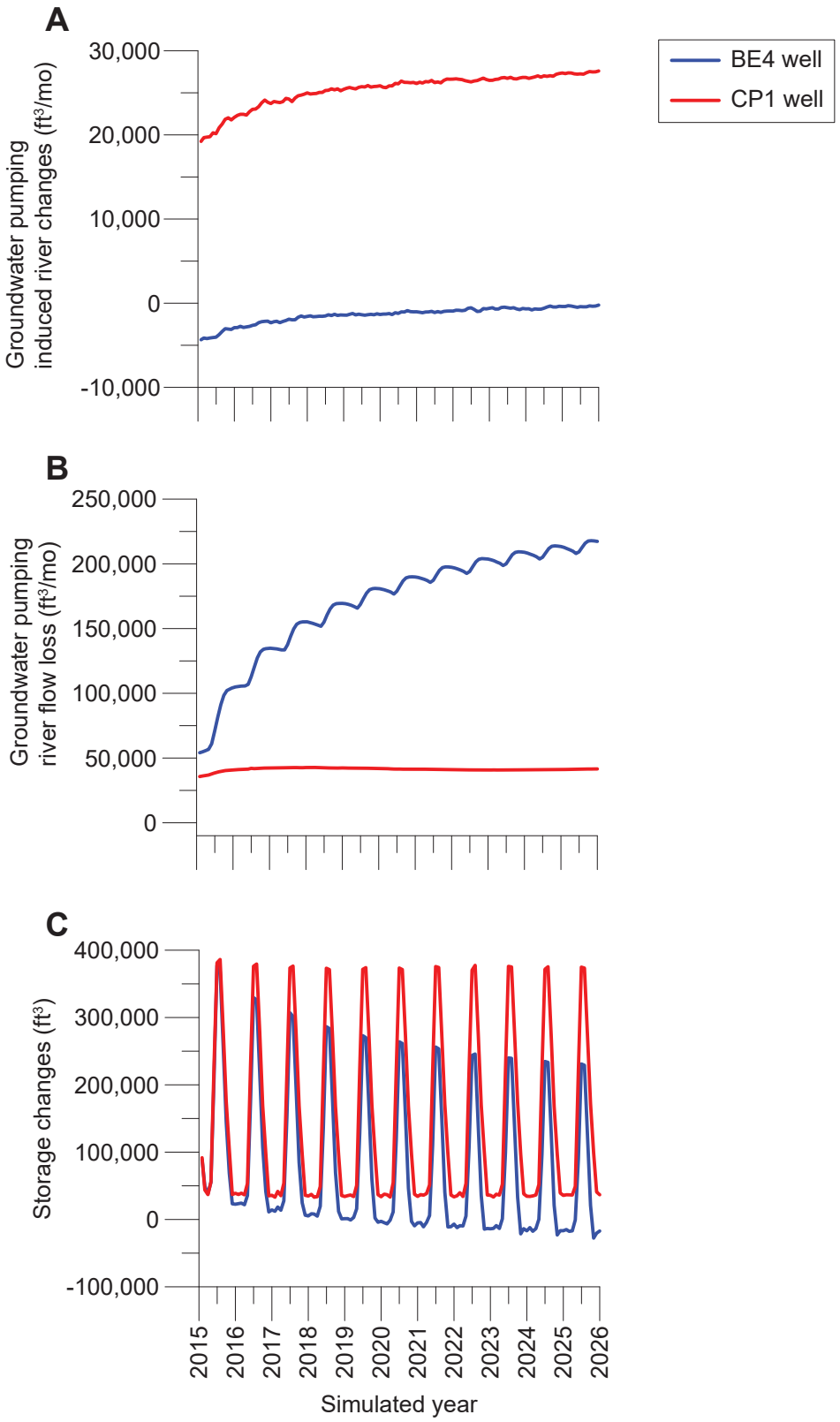

Figure 15. Graphs A and B illustrate the changes in stream (A) and river (B) loss from pumping north (CP1) or south (BE4) of the Central Park fault as compared to the baseline model with no pumping. Stream capture (A) is greater north of the fault, while river capture (B) is greater south of the fault. Storage changes are highly variable and reflect withdrawal and recharge as pumping demands increase and decrease seasonally (C). Positive values indicate a gain; negative indicate a loss.

and additional water is drawn from storage. This is likely due to the rapid availability of storage water and the slower recharge of storage from the river during months of decreased pumping (figs. 15B, 15C). Proximity of the pumping well to surface water causes immediate decrease in surface-water flows. Over time, however, the overall pumping-induced volume of losses will be the same; only the surface-water source changes.

Scenario 3: Pumping Offset

The transient 10-yr numerical model was used to determine the effects of mitigation using spring runoff located near the Yellowstone International Airport. This scenario used well BE3 pumping at a 5,000 acre-ft/yr (table 5, fig. 11) in layer 1, as for the other scenarios. The mitigation area is an array of 16 injection wells that simulate an infiltration pond equally applying a total of 5,000 acre-ft/yr to approximately 5 ft below the ground surface to simulate surficial recharge from a pond (location BE5). Two injection schedules were simulated. The first schedule applied the entire 5,000 acre-ft/yr in April, May, and June; the second schedule evenly distributed 5,000 acre-ft/yr throughout the year. High flows from spring runoff generally occur during these months and excess water is typically available during this time. Figure 16 shows the changes to the rivers, streams, and storage compared to the baseline model.

The first simulation involves mitigation only during spring runoff. This simulation showed a highly variable interaction with the rivers (fig. 16A). When water infiltration occurs over 3 mo in the spring, both groundwater storage and groundwater discharge to surface water increase. This indicates infiltration over a limited time increases aquifer storage by raising the water table (fig. 16C), but the elevated water table also increases the gradient and resulting flux to surface-water capture (i.e., streamflow increases; figs. 16A, 16B). The streams indicate a similar pattern to that of spring runoff infiltration, with surface-water capture increasing over time (fig. 16B). While the system would eventually reach equilibrium, with streamflow increasing as nearly all the injected water discharges to surface water, equilibrium was not reached during the 10-yr transient model run.

The second simulation involved offsetting pumping with a constant infiltration rate throughout the year. Storage changes closely followed the current annual pattern (fig. 16C), and smaller, steadier changes were simulated in surface-water capture (figs. 16A, 16B).

The location of the infiltration, placed near the spring creeks, affected the streams by increasing groundwater discharge to them. The volume of baseflow decreased slowly, indicating a new equilibrium would be reached at some point in the future with less loss to surface water than is modeled in the first 10 yr of infiltration.

The result of this scenario suggests steady, annual recharge to the aquifer is more likely to be retained in aquifer storage to offset pumping than a time-limited, high-volume influx, causing the overall change in storage to be near zero. The rapid spring infiltration site created a groundwater mound that did not dissipate quickly enough to avoid impacts to streams from subsequent groundwater pumping. The high-volume influx to the aquifer during spring runoff did not surcharge storage but discharged relatively quickly to surface water. The proximity of the infiltration area to surface water increased the likelihood of rapid discharge to surface water from the elevated water table. A distal location further from rivers or streams would increase storage of injected water rather than discharging to surface water.

Scenario 4: Timing and Location of Decreased Stream Flow

The transient 10-yr numerical model was used to determine stream and river reaches most influenced by pumping based on location. The pumping wells are north (CP1) and south (BE3) of the Central Park fault (fig. 11), where there are thin sediments north of the fault and thick sediments south of the fault. This scenario is designed to identify differences between the two sediment packages' influence on surface water. The volume of surface water in each stream segment was calculated over 10 yr of pumping without mitigation.

Figures 17 and 18 show the timing and location of surface-water reduction from individually modeled stream and river reaches over the 10-yr transient period. The model compares two 80 ft pumping wells that draw 5,000 acre-ft/yr; well CP1, located in shallow alluvial sediments north of the Central Park fault, and well BE3, south of the fault, in a zone of deeper

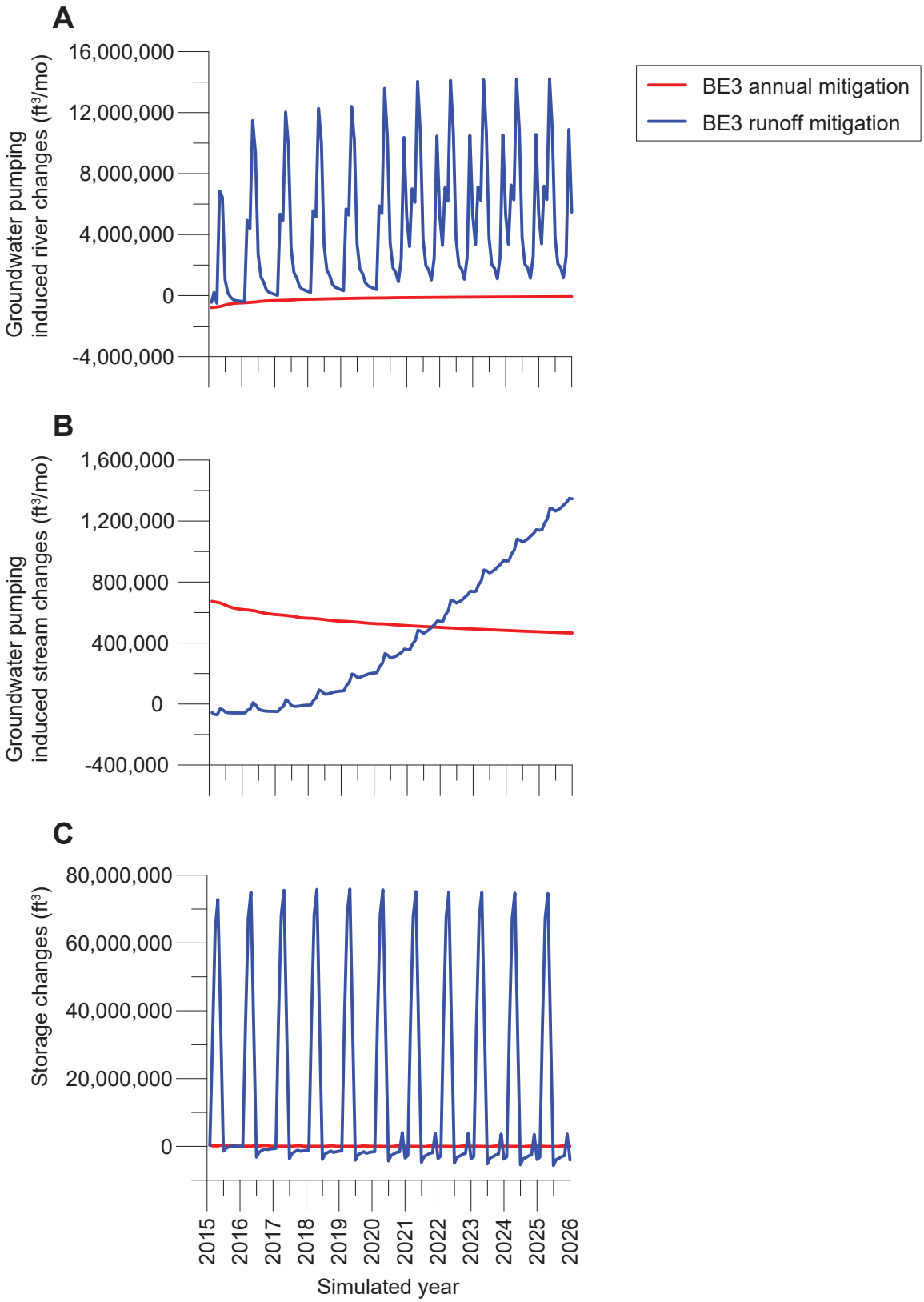

Figure 16. Graphs A and B illustrate the changes in river (A) and stream (B) loss from mitigation water injection as compared to the baseline model with no pumping. Mitigation is applied either annually as a constant inflow to the aquifer, or as seasonal runoff for 3 mo in the spring. River capture (A) and stream capture (B) offset much of the aquifer inflow in the runoff mitigation simulation, while changes to the river (A) and storage (C) are minimal using annual inflow. Positive values indicate a gain; negative indicate a loss.

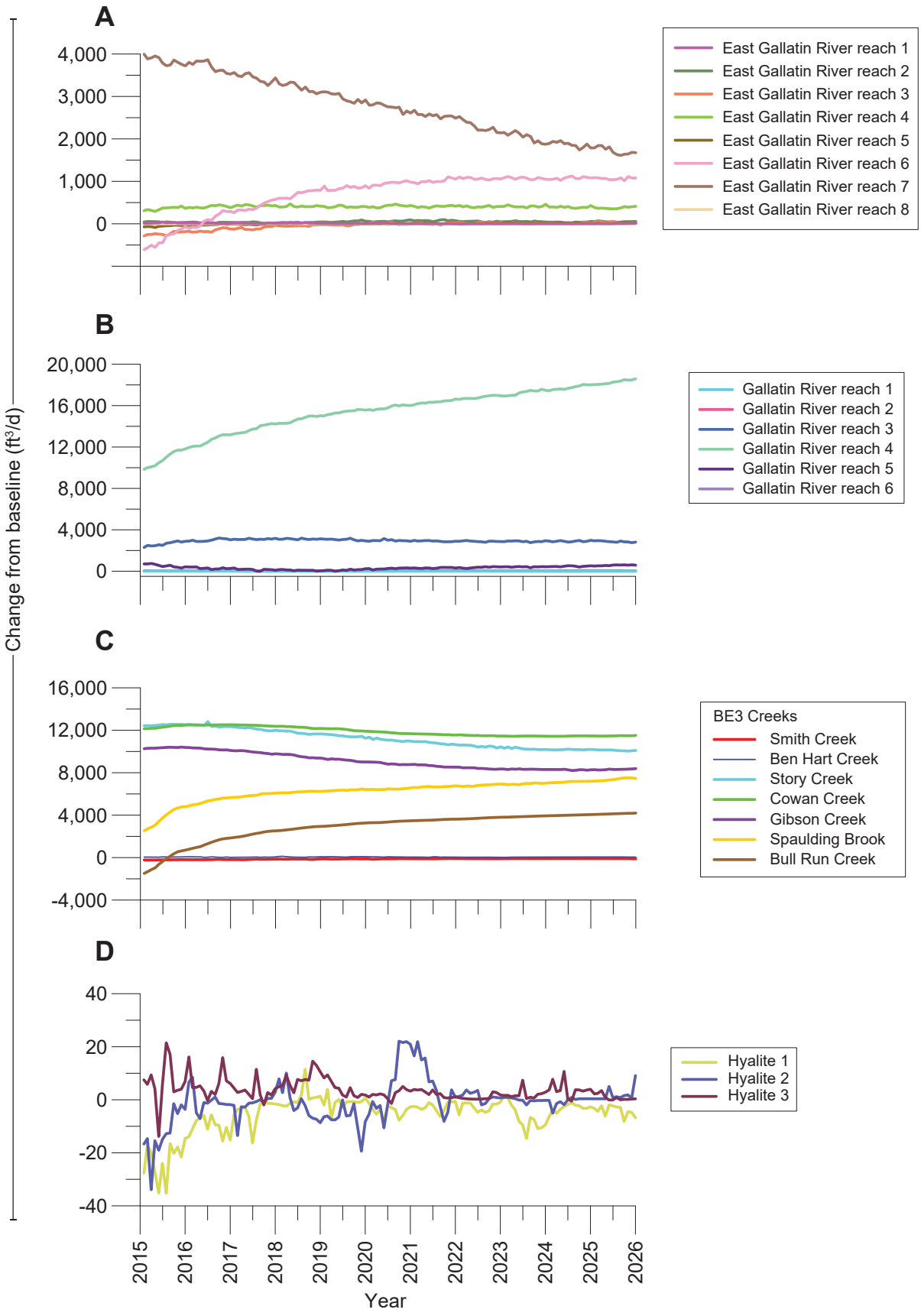

Figure 17. In Scenario 4, individual river reaches (A, B, and D) and stream reaches (C) are affected by a pumping well north of the Central Park fault. The direct connection between surface water and groundwater north of the fault caused most surface-water loss to come from the streams located near this well (C), while the adjacent reaches of the East Gallatin (A) and Gallatin Rivers (B) were responsible for part of the leakage.

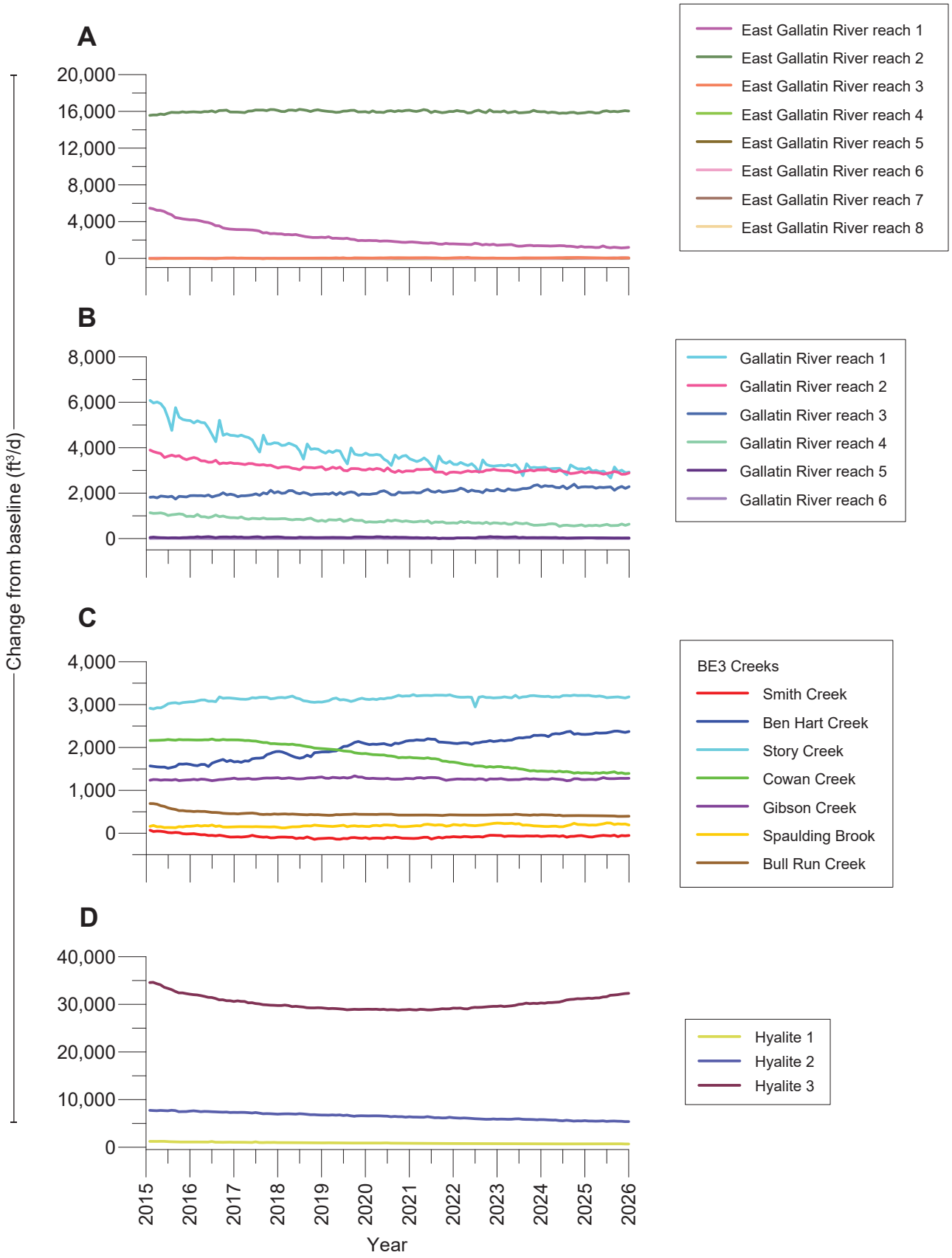

Figure 18. In Scenario 4, individual river reaches (A, B, and D) and stream reaches (C) are affected by a pumping well south of the Central Park fault. Hyalite Creek (D) and the East Gallatin (A) reaches directly adjacent to the pumping well were responsible for most of the induced stream loss, while the Gallatin River (B) and the smaller streams (C) lost smaller amounts.

alluvium. River reaches are numbered from the south end of the model domain and increase with the flow direction [example, East Gallatin 1 (EG1) begins at the south model boundary and East Gallatin 7 (EG7) ends at the confluence with the Gallatin River; fig. 11].

Pumping from well CP1 primarily affected reach 7 of the East Gallatin River (fig. 17A), reach 1 of the Gallatin River located directly west (fig. 17B), and from the smaller streams (Story, Cowan, and Gibson Creeks; fig. 17C). Well CP1 is closer to the springs that form the headwaters of the small streams, and pumping decreased flows in several of these streams. Hyalite Creek, which meets the East Gallatin upgradient from well CP1, showed the least effect (fig. 17D). The direct connection between surface water and groundwater north of the fault led to immediate and lasting decrease in surface-water flows near this well.

Streamflow decreases were more evenly spread across upstream reaches of the rivers (East Gallatin reaches 1 and 2 (fig. 18A); Gallatin River reaches 1, 2, and 3 (fig. 18B), with smaller changes induced in the creeks. Pumping of well BE3, located in the deeper alluvial sediments south of the fault, had a smaller (<3,500 ft^3/d) effect on the streams when compared to pumping from well CP1 (fig. 18D). Additionally, the flow rates in many reaches attained equilibrium more quickly compared to pumping from well CP1 (figs. 17, CP1 and 18, BE3), though Hyalite Creek reach 3 showed the greatest changes.

The results of this scenario suggest the distance between the pumping well and the surface-water body is the most important factor in determining induced changes to surface-water flows, as the cone of depression extends outward in all directions. While the depth of the pumping well may also be important, it was not examined in this scenario. The results of Scenario 1 suggest shallow wells may have a greater influence on surface water. Over time the reduction in groundwater discharge to surface water will become similar, but the surface-water reaches closest to the pumping well will be affected the most. Well BE3 had a more diffuse capture profile that leveled out to a constant rate more quickly, likely due to the availability of storage to offset immediate withdrawals and distance from surface-water bodies. Smaller streams with relatively low flow are more likely to cease flowing over time, especially in drier years, if a pumping well located nearby is completed in shallow sediments.

Sensitivity/Uncertainty

A sensitivity analysis that varied key numerical model parameters was conducted using the steady-state numerical model. Parameters altered included horizontal hydraulic conductivity in each layer and subarea. As multipliers were applied to the calibrated range, hydraulic conductivity was altered to exceed reasonable parameters based on the geology of the sediments. The wide variability of the river heads allowed for some hydraulic conductivities to fall within expected flows; however, the calibration was deemed geologically unreasonable.

A later version of the sensitivity analysis was performed on the transient 10-yr numerical model; however, altering variables within the transient numerical model caused destabilization and prevented MODFLOW convergence. This indicates the numerical model is stable within the expected range of hydraulic conductivities, particularly in the first layer. The transient numerical model seemed most sensitive to hydraulic conductivity and storage parameters, which prevented convergence.

Numerical Model Limitations

The Belgrade–Manhattan groundwater flow model is useful for determining the expected response of ground and surface water to new stresses; however, it has limitations. The superposition model was not calibrated to measured groundwater heads, and the surface-water flows and stages that were used as calibration targets have wide ranges throughout the study period. For these reasons, the model is best suited to assess the expected magnitude and/or location of influence. The model should be used in superposition mode, to determine changes that may occur within the model domain compared to the base case.

The subareas that fall within the valley floor were the primary focus of the modeling, with distal areas at the boundaries reaching into the surrounding benches and foothills. Simulation of applied stresses outside of the floodplain may be subject to boundary influences and, therefore, not accurately represent changes to the system. The model is well suited to simulate new stresses within the Manhattan, Central Park, and Belgrade subareas, which was the focus area of model calibration.

Analytical Model

Hypothetical pumping wells installed in the transient 1-yr numerical model compared well to the analytical model, despite heterogeneity in the hydraulic conductivity of the numerical model. At the same location as the River Rock subdivision aquifer test, a pumping well discharging 50,000 and 500,000 ft^3/d displayed similar drawdown to the analytical model. Similar pumping tests performed in multiple locations indicated similar results. Details are provided in appendix A.

DISCUSSION

The MODFLOW models suggest water is physically available for pumping in most of the simulation (or scenario) locations; however, the proximity of pumping to surface-water bodies dictates the timing and magnitude of pumping-induced reductions in discharge to surface water. These models indicate that effects to groundwater at a distance are comparable whether pumped as a single well or a well field. Surface-water effects will be greatest in the reaches nearest pumping. The overall volume of surface-water changes is nearly equivalent in the different pumping approaches (table 8); however, the timing of those effects varies.

Deeper alluvial sediments, particularly the coarser Quaternary sediments, have a higher relative storage capacity and transmissivity than the thin, shallow sediments, which allows for greater well yields. For this reason alone, the preferred location for any large-scale municipal water supply is south of the Central Park fault. The aquifer's ability to capture and store groundwater is greater in the deep sediments, allowing for any mitigation efforts to be more successful in the Belgrade subarea.

The aquifer displays a direct connection to surface water; consequently, both mitigation and pumping will directly influence surface-water flows. Pumping at locations more distant from surface water will decrease surface-water flows over time; however, the more immediate depletion is from groundwater storage. Similarly, mitigation applied to the aquifer increases groundwater discharge to surface water. When a large pulse of water is applied, a large groundwater

Table 8. Summary table of predictive scenarios.

Scenario	Model	Simulation Design	Simulation Results
Scenario 1	Steady-state	Compares a single well pumping 5,000 AF/y to an 81-well array pumping 5,000 AF/y (located at site BE4)	Cones of depression indistinguishable at 1 mi from center of array vs. pumping well
			Stream capture volume is virtually identical
	Transient 10 yr		Volume of water removed determines surface-water capture, not the number pumping wells
Scenario 2	Steady-state	Compares a single pumping well in low HK sediments (BE1) to a single pumping well in high HK sediments (BE2)	High HK aquifer zones create a steeper cone of depression than low HK zones
			High HK aquifer zones create a narrower cone of depression than low HK zones
	Transient 10 yr	Compares a single pumping well in shallow sediments (CP1) to a single pumping well in deeper sediments (BE4) with similar HK	Pumping wells located nearer surface water induce greater surface-water capture than distant wells
			Pumping wells in shallow sediment packages induce greater surface-water capture over time
Scenario 3	Transient 10 yr	Compares mitigation of pumping well (BE3) through an infiltration pond (BE5); mitigation occurs uniformly throughout the year vs. during spring months	More mitigation water is captured by groundwater storage when applied uniformly throughout the year than when applied over a 3-mo period
			A cone of injection causes surface-water capture and prevents water from entering groundwater storage when mitigation water is applied over 3 mo
Scenario 4	Transient 10 yr	Compares the timing and location of surface-water capture from pumping well CP1 in shallow alluvium and well BE3 in a deeper sediment package	Proximity to surface water determines the amount of surface-water capture induced by pumping
			Deeper sediment packages create a more diffuse surface-water capture profile and reach equilibrium more rapidly when pumped

mound increases the hydraulic gradient and subsequent discharge of groundwater to surface water. A slower, more gradual influx increases retention time in the aquifer, retaining groundwater in storage that discharges to surface water over a longer period.

Distance from surface water and depth of the alluvial sediments are the two key factors in determining the influence pumping will have on streams and that infiltration will have on the aquifer. For this reason, the Belgrade subarea appears most conducive for successful municipal water development, with the Central Park, Manhattan, Camp Creek Hills, and Bozeman subareas being considered feasible for lower volume pumping.

Conclusions and Recommendations

The groundwater model developed for this project provides a useful tool for estimating the changes to surface water and groundwater from pumping and infiltration. Model results can inform decisions about placement of new PWS wells and can help predict the timing and magnitude of impact to groundwater levels and surface-water capture.

The design of this MODFLOW model makes it possible for a user to understand the effects of individual reaches of river or stream and estimate the impacts of new stresses. The model could be used to simulate effects within individual zones in each of the scenarios, to further investigate the influence of the geology on water capture.

Additional aquifer tests, particularly in the deeper Tertiary units that are rarely tapped for groundwater pumping, would improve the calibration of the numerical model. Monthly monitoring of head and stage near the spring creeks south of the Central Park fault would improve the numerical model's ability to predict the impacts to surface water and improve the numerical model's predictive capability.

The numerical model is a useful tool for planning water development or movement. These models can be used to estimate the cone of influence from a hypothetical pumping well using the hydraulic properties near the well.

ACKNOWLEDGMENTS

This study benefited from the assistance of the many landowners and residents of the Gallatin Valley who provided access to their property and wells. Walt Sales provided information on the hydrologic system and invaluable assistance in background, access, and historic knowledge. The Gallatin Local Water Quality District aided in both monitoring and access. The Bozeman office of the Montana Department of Natural Resources aided in accessing water rights and their data sharing is appreciated.

The Groundwater Assessment Program's long-term data monitoring provided an essential basis for this study. GWIP employees Tom Michalek, Dean Snyder, Mark Schaffer, and Bill Henne assisted in data collection and processing. Montana Tech students Taylor Stipe, Amber Gruel, and Emily Welk assisted with data collection and data management. Andy Bobst and Nick Banish provided invaluable insight and constructive reviews of this manuscript. Susan Smith and Susan Barth from the MBMG assisted with figure preparation, editing, and report layout.

REFERENCES

Aquaveo, LLC, 2014, Groundwater Modeling System (GMS), version 10.0.2.

ASTM International, 2008, Standard test method for (field procedure) withdrawal and injection well testing for determining hydraulic properties of aquifer systems, 3rd ed.: ASTM International, West Conshohocken, Penn., 5 p.

ASTM International, 2010, Determining subsurface hydraulic properties and groundwater modeling, 3rd ed.: ASTM International, West Conshohocken, Penn., 358 p.

ASTM International, 2012, Standard test method for (analytical procedure) determining transmissivity, storage coefficient, and anisotropy ratio from a network of partially penetrating wells, 4th ed.: ASTM International, West Conshohocken, Penn., 11 p.

Bear, J. (1979). Hydraulics of groundwater, McGraw-Hill, New York.

Bear, J., and Cheng, A., 2010, Modeling groundwater flow and contaminant transport: Dordrecht, Springer, doi: 10.1007/978-1-4020-6682-5

Breuninger, R.H., and Mendes, T.M., 1993, Summary report: Groundwater availability in the proposed Summer Ridge subdivision, Gallatin County, prepared by Morrison-Maierle, Inc., 20 p.

Calver, A. 2005, Riverbed permeabilities: Information from pooled data: Ground Water, v. 39, no. 4, p. 546–553.

Carstensen, J., 2008, Ground-water Modeling Effort For Evaluation of Zone of Influence and Stream Depletion/Accretion: Utility Solutions, LLC HBB831 Application, 28 p.

Custer, S.G., Donohue, D., Tanz, G., Nichols, T., Sill, W., and Wideman, C. 1991, Ground-water potential in the Bozeman-Fan subarea, Gallatin County, Montana: Final report of research results to Water Development Bureau: Montana Department of Natural Resources and Conservation, 141 p.

Custer, S.G., and Schaffer, M.A., 2009, Assessment of the interaction between ground water and the Gallatin River in the Four Corners area, Gallatin County, Montana—Final report to the renewable resource grant program, Montana Department of Natural Resources and Conservation, for grant RRG 06-1242: Bozeman, Mont., Montana State University Earth Sciences Department, 35 p.

Department of Natural Resources and Conservation (DNRC), 2011, General water use requirements submitted to the Water Policy Interim Committee for the September 13, 2011 meeting, available at http://leg.mt.gov/content/Committees/ Interim/2011-2012/Water-Policy/Meeting-Documents/September-2011/water-use-table.pdf [Accessed July 2018]

Department of Natural Resources and Conservation (DNRC), 2016, Montana's Basin Closures and Controlled Groundwater Areas. Water Resource Division, Water Rights Bureau, updated 2016. Available online at https://www.dnrc.mt.gov/_docs/water/Montana-Basin-Closures-and-Controlled-Groundwater-Areas-6_2_2016-modified-RO-Comments.pdf [Accessed January 2023]

Dixon, S.A., and Custer, S.G., 2002, Driller specific capacity as a measure of aquifer transmissivity and a test of the hydrogeologic units in the Gallatin Local Water Quality District, Gallatin County, Montana: Bozeman, Mont., M.S. Thesis, Montana State University, 127 p.

Doherty, J. (2003). Ground water model calibration using pilot points and regularization. *Ground Water, 41*(2), 170-177.

Doherty, J., 2010, PEST model-independent parameter estimation user manual, 5th ed.: Brisbane, Australia, Watermark Numerical Computing, 336 p., available at http://www.pesthomepage.org [Accessed May 2011].

Driscoll, F.G., 1986, Groundwater and wells: St. Paul, Minn., Johnson Div, Retrieved from http://mtproxy.lib.umt.edu:3048/login?url=https://www.proquest.com/books/groundwater-wells/docview/2359366633/se-2 [Accessed January 2023].

Dunn, D.E., 1978, Ground water levels and ground water chemistry, Gallatin Valley, Montana: Blue Ribbons of the Big Sky Country Area wide Planning Organization report, #11, 62 p.

English, A.R., 2018, Evaluation of potential high-yield groundwater development in the Gallatin Valley, Gallatin County, Montana: Montana Bureau of Mines and Geology Open-File Report 698, 22 p., 2 sheets.

Gaston Engineering, 1996, Engineer's report for the aquifer testing at the Spirit Hills subdivision: Bozeman, Mont., unpublished report, 9 p.

Groundwater Information Center (GWIC), 2016, Montana Bureau of Mines and Geology Groundwater Information Center, available at http://mbmggwic.mtech.edu/sqlserver/v11/menus/menuProject.asp?mygroup=GWIP&myroot=BWIPMN&ord=1& [Accessed January 2023].

Hackett, O.M., Visher, F.N., McMurtrey, R.G., and Steinhilber, W.L., 1960, Geology and groundwater resources of the Gallatin Valley, Gallatin County, Montana: U.S. Geological Survey Water-Supply Paper 1482, 282 p.

Harbaugh, A., Banta, E., Hill, M., and McDonald, M., 2000, MODFLOW-2000, The U.S. geological survey modular ground-water model—User guide to modularization concepts and the ground-water flow process: U.S. Geological Survey Open-File Report: 2000-92, 121 p.

Hay, J.E., 1997, An investigation of groundwater recharge along the western flank of the southern Bridger Range, southwestern Montana: Bozeman, Mont., M.S. thesis, Montana State University, 161 p.

Kaczmarek, M., 2003, Groundwater availability for alluvial wells in the Four Corners area, Gallatin County, Montana: Montana Department of Natural Resources and Conservation, Helena: Utility Solutions, LLC, 36 p.

Kendy, E., and Bredehoeft, J.D., 2006, Transient effects of groundwater pumping and surface-water irrigation returns on streamflow: Water Resources Research, v. 42, no. 8, 11 p.

Lohman, S.W., 1979, Ground-water hydraulics: U.S. Geological Survey Professional Paper, 70.

Lonn, J., and English, A., 2002, Preliminary geologic map of the eastern part of the Gallatin Valley, Montana: Montana Bureau of Mines and Geology Open-File Report 457, 17 p., 1 sheet, 1:50,000.

Michalek, T., and Sutherland, M., 2020, Hydrogeologic investigation of the Four Corners area, Gallatin County, Montana: Interpretive report: Montana Bureau of Mines and Geology Open-File Report 735, 74 p.

Murdoch, H.E., 1926, Irrigation and drainage problems in the Gallatin Valley: University of Montana Agricultural Experiment Station, Bozeman, Mont., 36 p.

National Agricultural Imagery Program (NAIP), 2015, Natural-Color Aerial Photos of Montana, 2011, available at http://nris.mt.gov/gis/ [Accessed June 2017].

Schaffer, M.A., 2011, Ground-water discharge and aquifer recharge zones near four corners, Gallatin County, Montana: Bozeman, Mont., M.S. Thesis, Montana State University.

Slagle, S.E., 1995, Geohydrologic conditions and land use in the Gallatin Valley, southwestern Montana, 1992–1993: U.S. Geological Survey Water Resources Investigations Report 95-4034, 2 sheets, scale 1:100,000.

Stone, H.L., 1968, Iterative solution of implicit approximations of multidimensional partial differential equations: Journal of the Society for Industrial and Applied Mathematics, v. 5, p. 530–558.

Theis, C.V., 1935, The relation between the lowering of the piezometric surface and the rate and duration of discharge of a well using ground-water storage: American Geophysical Union Transactions, v. 16, p. 519–524.

U.S. Census Bureau, 2023, QuickFacts, Gallatin County, Montana, available at https://www.census.gov/quickfacts/gallatincountymontana [Accessed January 2023].

U.S. Geological Survey (USGS), 1999, National elevation dataset (NED), available at http://ned.usgs.gov/ [Accessed July 2013].

U.S. Geological Survey (USGS), 2017a, USGS 06052500 Gallatin River at Logan Mont., available at https://waterdata.usgs.gov/mt/nwis/dv/?site_no=06048650&PARAmeter_cd=00060,00065 [Accessed December 2017].

U.S. Geological Survey (USGS), 2017b, USGS 06048650 E Gallatin R ab Water Reclamation Fa nr Bozeman MT., https://waterdata.usgs.gov/mt/nwis/dv/?site_no=06052500&PARAmeter_cd=00060,00065 [Accessed December 2017].

Vuke, S.M., 2003, Geology of western and northern Gallatin Valley, southwestern Montana: Montana Bureau of Mines and Geology Open-File Report 481, 40 p., 1 sheet, scale 1:50,000.

Vuke, S.M., Lonn, J.D., Berg, R.B., and Schmidt, C.J., 2014, Geologic map of the Bozeman 30’ x 60’ quadrangle, southwestern Montana: Montana Bureau of Mines and Geology Open-File Report 648, 44 p., 1 sheet, scale 1:100,000.

APPENDIX A:

NUMERICAL GROUNDWATER MODEL DETAILS

APPENDIX A. NUMERICAL GROUNDWATER MODEL DETAILS

A superposition model was developed to understand the potential changes to surface water and groundwater based on hypothetical pumping scenarios in different locations within the study area (main text, fig. 1). Public water supply is in increasing demand as the population increases, and the location of new groundwater supplies depends on the ability to offset that demand in the closed basin. The superposition model allows for the model to remove any unknown stresses from the equation and look only at the effects of new stresses (i.e., pumping) to surface water and groundwater.

Analytical Model

The analytical model uses Microsoft Excel 2016, to solve the Theis distance-drawdown equation presented by Lohman (1979; eq. 45, 48). This analytical model allows the user to define storage, transmissivity, time, and discharge to solve the mathematical equation for drawdown at a given distance from the pumping source.

The analytical model is limited in function to determining the cone of depression at some distance from a pumping well. The model solves the Theis nonequilibrium method (Theis, 1935) with the Lohman (1979) well function modification. The analytical model also acts as a verification tool for the numerical groundwater model.

The analytical model was developed based on observed and published hydrogeologic properties of the aquifer in the study area. It uses the Theis (1935) distance-drawdown equation to calculate water levels at differing distances from the pumping well. The discharge rates can also be varied to determine drawdown at different distances from the pumping well. The model assumes a constant rate of flow through a homogeneous, uniform thickness aquifer of infinite extent. Further assumptions include instant release of water from storage in a non-leaking confined aquifer. The Lohman (1979) modification includes well function to allow for vertical water flow and partially penetrating wells in the aquifer.

Groundwater Modeling Software

Groundwater Modeling System (GMS) software (Aquaveo, 2014; all references in main text) provided a graphical user interface for developing a MODFLOW 2000 numerical groundwater flow model. MODFLOW 2000 is a widely accepted numerical groundwater flow model developed by the U.S. Geological Survey (Harbaugh and others, 2000). MODFLOW is a modular finite-difference flow model, used to simulate the flow of groundwater through porous media. This numerical model used GMS version 10.0.2, built August 20, 2014, in conjunction with MODFLOW 2000 version 1.19.01, compiled March 25, 2010. The Strongly Implicit Procedure (SIP1) solver (Stone, 1968) and automated parameter estimation (PEST v. 13.0; Doherty, 2010, 2013) were used in conjunction with MODFLOW software.

Numerical Model Construction

The numerical model grid was created in GMS using the North American Datum (NAD) 1983 State Plane coordinates (table A1). The numerical model dimensions are in international feet. The grid is cell-centered with an x origin of 88,255 ft, a y origin of 521,936, and a z origin of 3,996. A rotation angle of 75

Table A1. Details of the numerical model grid.

X origin:	1,497,726 ft
Y origin:	521,936 ft
Z origin:	3,996 ft
Length in X:	88,255 ft
Length in Y:	85,307 ft
Length in Z:	500 ft
Rotation angle:	15
AHGW X origin:	1,475,646 ft
AHGW Y origin:	604,336 ft
AHGW Z origin:	4,496 ft
AHGW Rotation angle:	75
Minimum scalar:	4,092
Maximum scalar:	4,626
Num cells i:	285
Num cells j:	295
Num cells k:	5
Number of nodes:	507,936
Number of cells:	420,375
No. Active cells:	275,400
No. Inactive cells:	144,975

degrees was specified to orient the grid in the approximate north–northwest direction of groundwater flow in the valley. Selected potentiometric contours surrounding the valley determined the active cell coverage within the grid (fig. A1).

Grid cells are square in plan view, approximately 299 ft in each horizontal direction. The surface of the numerical model was kriged from all surveyed elevations available in the GWIC database. This surface was created due to large discrepancies between the National Elevation Dataset (NED; USGS, 1999) and project-surveyed elevations. The active numerical model grid covers an area of approximately 177 mi^2. The focus of this numerical model is the valley floor, primarily adjacent to and between the two forks of the Gallatin River. Any use of this numerical model should be limited to that area.

The numerical model includes five layers. Layer one is approximately 100 ft thick below the surface at the valley floor. The areas to the east and west of the

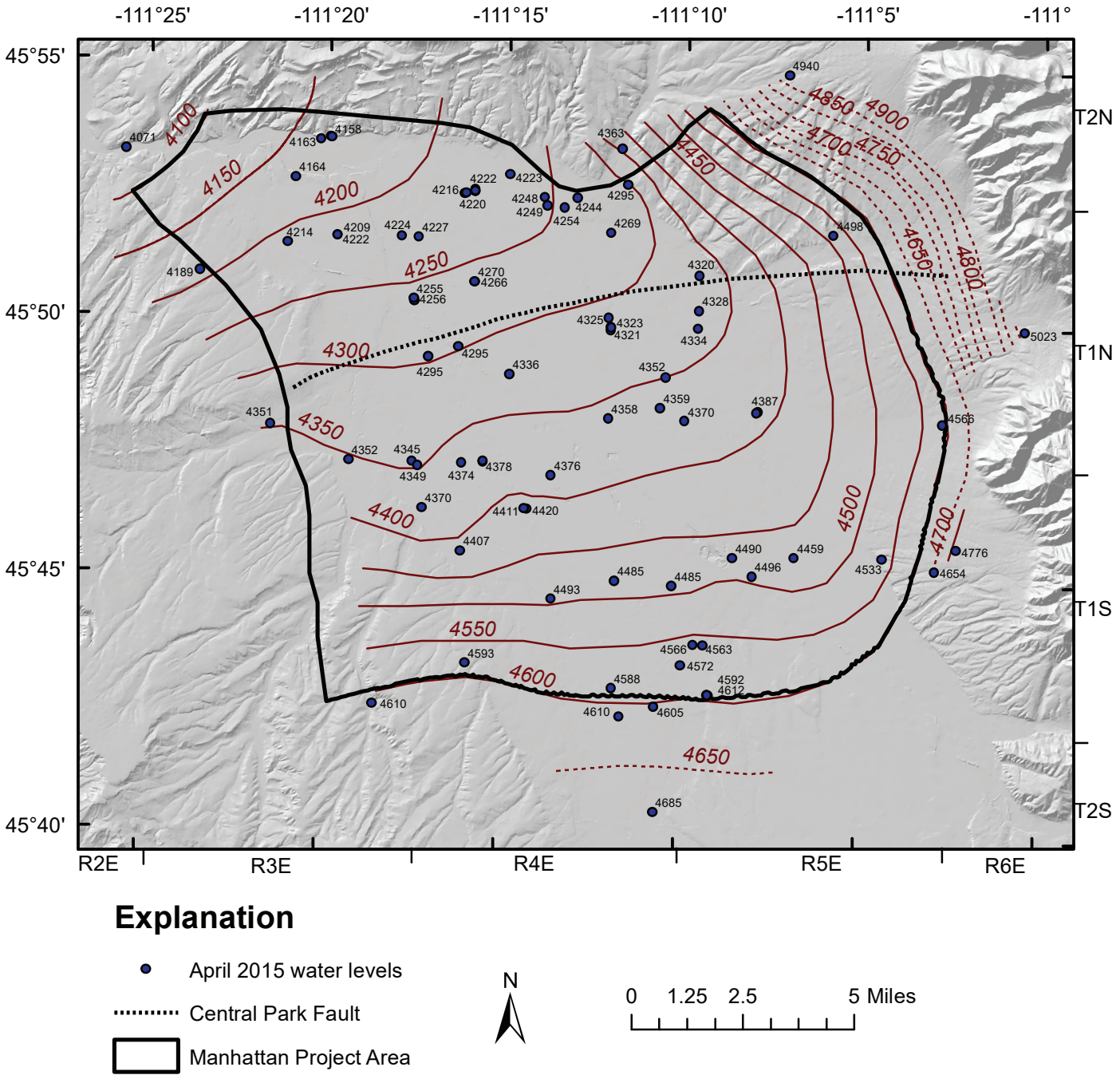

Figure A1. The potentiometric map developed from measured April 2015 water levels was used to define the numerical model boundaries. No flow boundaries run perpendicular to potentiometric contours, while constant head boundaries were matched to the 4,100 and 4,600 ft contours.

valley are steeply sloping. Due to these elevations, the bottom of layer one was flattened outside of the valley floor. This flattening accommodated groundwater properties assigned in MODFLOW that replicate the groundwater surface. Within the valley floor, layer one maintains a consistent thickness of 100 ft. These conditions are represented in the east–west cross-section of the numerical model grid (main text, fig. 9).

The thickness of layer one ranges from 96 ft to 513 ft beyond the valley floor area. The areas outside of the valley floor are not germane to the numerical modeling scenarios and act only as boundary conditions. Layers two, three, four, and five are all 100 ft thick with elevations derived from the bottom of layer one. These layers are not intended to represent the vertical depth of the units; rather the applied hydraulic conductivity is averaged with depth to represent the geologic matrix governing groundwater flow. The layering of the numerical model is necessary to distinguish vertical conductivity zones; they are reflective of decreasing HK with depth.

Numerical Model Boundaries

The numerical model boundaries are distant boundaries, which means that the boundaries are placed at such a distance as to prevent boundaries from interfering with calculations performed in the valley. A constant head boundary at the 4,600 ft potentiometric contour bounds the numerical model to the east and south. This contour extends into the Eastern Benches to represent the recharge from flow out of the Bridger Mountains to the east. The contour continues south along Hulbert Road, where recharge derived from the Gallatin Range and the Spanish Peaks flows northwest through the valley. Monthly potentiometric surfaces show very little seasonal fluctuation in this contour, so it was kept constant in the transient models.

The numerical model slopes northwest toward the confluence of the Gallatin River and the East Gallatin River, where the basin drains near Logan. A constant head at 4,100 ft also represents this outflow boundary to the northwest. The north and west boundaries both run parallel to flow paths, creating no-flow boundaries to enclose the numerical model area. Although some flow may be moving through fractures in the Horseshoe Hills bedrock, it is negligible to the results of this numerical model. All boundaries are located far enough away to eliminate influence on drawdown and surface-water changes from applied stresses. Additionally, constant head boundaries act as zero-potential boundaries in that when superimposed upon one another, the constant heads will affect zero drawdown (Bear, 1979).

Surface water, considered as an interior source or sink rather than a boundary, nonetheless crosses the boundaries of the numerical model in four locations. Inflow from Hyalite Creek, the East Gallatin River, and the Gallatin River enters the numerical model through the southern boundary. Outflow crosses the western constant head boundary after the East Gallatin and Gallatin Rivers merge. More detail on the rivers and other surface-water bodies are provided in the "Sources and Sinks" section.

Hydraulic Properties

This numerical model uses the hydraulic conductivity (K) of the aquifer and streambed conductance (C) of surface water to control flow through the aquifer and groundwater–surface water exchange, respectively. Hydraulic conductivity describes the ease of water flow though the aquifer. Low K indicates high resistance to flow and is generally associated with slow-moving water, while high K relates to low resistance to flow and generally faster moving water (main report, table 1). In unconsolidated sediments, low K generally suggests finer-grained materials such as fine sand or silt, whereas high K indicates coarser-grained materials such as coarse sand and gravel. River or streambed conductance is similar to K in controlling water movement, but accounts for the geometry of the streambed in addition to the K of the streambed sediments.

The hydraulic characteristics of each layer are representative of the geology and hydraulic conductivity of those areas. In the valley floor, coarse-grained Quaternary and Tertiary alluvium are representative of the floodplain between the Gallatin and East Gallatin Rivers (Vuke and others, 2014). Well logs describe these sediments as a mix of coarse cobbles to clay-rich sands and silts. The valley fill is divided into zones of alluvial or fluvial sediments (English, 2018). Tertiary sediments are commonly, but not always, weakly cemented.

Fine Tertiary sediments are present at greater depths, although the Quaternary/Tertiary boundary varies by location. North of the Central Park fault,

finer and more compacted Tertiary sediments appear at less than 100 ft, while south of the fault fine Tertiary sediments occur at greater depths (main text, fig. 8). Layering of the numerical model reflects shallow, fine Tertiary sediments north of the fault and thicker, coarse sediments south of the fault. The numerical model uses staggered zones of horizontal conductivity (HK) at varying depths to reflect the hydraulic characteristics of the fill.

Sources and Sinks

Surface-water data from stations at the Gallatin River at Logan (USGS station 06052500) and the East Gallatin River near Bozeman (USGS station 06048650) were used, as well as streamflow data, hydraulic conductivity, and transmissivity information collected for this study. Gains to groundwater (sources) and losses from the aquifer (sinks) occurred along various surface-water reaches.

Hyalite Creek, the East Gallatin River, and the Gallatin River were simulated using the MODFLOW river package (RIV). This package incorporates observed head values for each reach of the rivers over the period of record. The river package calculates the gains and losses to the river reach based on streambed conductance, aquifer properties, and the relationship between stream stage and groundwater head. Each measurement location is entered in GMS as a node with an elevation for stage and river bottom based on surveyed project monitoring locations (table A2). GMS populates the intermediate MODFLOW river geometry based on the elevations assigned to these nodes. In GMS, these river segments are termed arcs. The river arcs follow the approximate course of the

Table A2. River (RIV) elevations and steady-state stage.

GWIC ID[a]		Site	Stage (ft)				Bottom Elevation	Top Elevation
			Low[e]	High[e]	avg	Change		
257400	[c]	Hyalite Creek–Hulbert Road	N/A	N/A	4,605.6	N/A	4,602.6	4,601.6
257394	[a]	Hyalite Creek–Valley Center	4,561.8	4,565.7	4,563.8	3.9	4,560.8	4,559.8
257396	[a]	Hyalite Creek–Frontage Rd	4,495.5	4,499.2	4,497.4	3.7	4,494.5	4,493.5
6048650	[d]	E Gallatin–Water Reclamation	4,627.8	4,631.2	4,629.5	3.4	4,626.8	4,625.8
264841	[a]	E. Gallatin–Dry Creek Rd	4,323.8	4,327.0	4,325.4	3.2	4,322.8	4,321.8
265047	[c]	E. Gallatin–Swamp Rd	4,269.1	4,270.2	4,269.7	1.1	4,268.1	4,267.1
262900	[a]	E. Gallatin–Dry Creek School Rd	4,249.3	4,252.2	4,250.8	2.9	4,248.3	4,247.3
265053	[a]	E. Gallatin–W. Dry Creek Rd	4,239.6	4,242.4	4,241.0	2.8	4,238.6	4,237.6
265035	[b]	E. Gallatin–Spaulding Bridge	4,222.9	4,224.1	4,223.5	1.2	4,221.9	4,220.9
258311	[b]	E. Gallatin–Penwell Bridge	4,385.9	4,390.7	4,388.3	4.8	4,384.9	4,383.9
257433	[a]	E. Gallatin–Gallatin River Ranch	4,157.5	4,163.0	4,160.3	5.5	4,156.5	4,155.5
6052500	[d]	Gallatin River–Logan MT	4,090.2	4,095.1	4,092.7	4.9	4,089.2	4,088.2
N/A	[c]	Gallatin River–inflow	N/A	N/A	4,595.8	N/A	4,591.4	4,590.4
257457	[a]	Gallatin River–Cameron Bridge	4,499.4	4,506.2	4,502.8	6.8	4,498.4	4,497.4
257355	[a]	Gallatin River–Amsterdam Rd	4,427.7	4,433.2	4,430.5	5.5	4,426.7	4,425.7
257356	[a]	Gallatin River–Frontage Rd	4,294.4	4,300.6	4,297.5	6.2	4,293.4	4,292.4
257458	[a]	Gallatin River–Dry Creek Rd	4,226.1	4,233.1	4,229.6	7.0	4,225.1	4,224.1
257431	[a]	Gallatin River–Nixon Gulch	4,154.0	4,159.1	4,156.6	5.1	4,153.0	4,152.0

[a]Data taken from SWAMP website.

[b]Data taken from GWIC website and corrected for MP.

[c]Estimated from nearest measured location elevation.

[d]USGS gaging station.

[e]1/1/2010–5/1/2017 or period of record.

river as visible in the 2015 National Agricultural Imagery Program (NAIP) aerial imagery.

The river arcs may act as both a source and a sink to the aquifer. The gain or loss from an arc is dependent on the adjacent water table elevation and conductivity of the streambed. Streambed conductance is calculated from the width of the stream and the thickness of the sediments underlying the stream. The calculation for streambed conductance (C) is:

$$C = (HK/b)w,$$

where C is streambed conductance; HK is streambed permeability; b is streambed thickness; and w is width.

Where the thickness of the streambed is unknown, b is set to a thickness of 1 ft. Stream widths are defined at the node where field measurements were taken. The range of streambed permeability for similar streams was taken from Calver (2005). Flow measurements from 18 locations along these reaches determined the expected range of gains and losses along these river cells.

The MODFLOW drain package (DRN) simulated groundwater losses from spring creeks emerging near the Central Park fault, which acted exclusively as sinks. Spaulding Brook, Gibson, Cowan, Story, Ben Hart, Bull Run, lower Smith, and Thompson Creeks discharge entirely within the study area. The drain package acts similarly to the river package in design; however, the drain package models only water lost from the aquifer (i.e., negative flow). GMS numerically models the nodes and arcs in the drain package similar to the river package, basing gains and losses on the elevation of the cell. Stage data are not considered in the drain package since only water loss from the aquifer is calculated. Elevations at the drain nodes were calculated from surface elevations mapped in the numerical model where they were not surveyed for the project (table A3).

Limited flow information on the creeks has demonstrated a hydraulic connection to the aquifer. As coarse hydraulic media thins north of the fault, these spring-fed creeks emerge to discharge water from the aquifer to the rivers. Flow measurements taken near the point where they discharge into the East Gallatin River were used as calibration targets to calibrate the numerical model. Since these streams begin within the numerical model domain, the overall flow is exclusively a loss from the aquifer.

Another groundwater sink in the numerical model is groundwater extraction for potential public water supply during pumping scenarios.

Numerical Model Calibration

The steady-state numerical model considered surface-water interactions with the aquifer and the hydraulic conductivity of the sediments governing groundwater flow. Calibration criteria focused on the geologic understanding of the aquifer and surface-water gains and losses. Water table elevations in select locations pertinent to predictive simulations were used qualitatively to assess the closeness of the simulated water table; however, heads were not quantitatively used in the PEST objective function.

The numerical model was considered calibrated when the hydraulic conductivities of each layer and subarea were reflective of the geologic understanding and the surface-water segments were within the measured flows. A combination of zonal and pilot point PEST was used to determine the optimal K array for each subarea and layer. The conductivities were constrained by the aquifer properties where available, and where unavailable, K was constrained by the author's geologic understanding of the system.

Table A4 shows the constraints placed on each subarea in each layer to define the calibrated hydraulic conductivity. The steady-state numerical model is calibrated to acceptable ranges of horizontal and vertical hydraulic conductivity and surface-water gains/losses (main text, tables 1 and 2). Streamflow gains and losses to the aquifer from the East Gallatin and Gallatin Rivers, Hyalite Creek, and five spring creeks over the course of the 2015 water year also served to calibrate the numerical model.

Assuming a thickness of 100 ft within the focus area, the calibrated conductivity values fall within the reported transmissivities of each zone (English, 2018; Hackett and others, 1960; Breuninger and Mendes, 1993; Kaczmarek, 2003; Gaston, 1996; Hay, 1997; Carstarphen, 2008; Kendy and Bredenhoeft, 2006).

Numerical Model Verification

The results from three aquifer tests were used to verify the numerical model (main text, fig. 5). The

Table A3. Streambed conductance for surface-water reaches (RIV and DRN model arcs).

Reach	HK low	HK high	w	b	C_{low} (ft/d)	C_{high} (ft/d)	C_{ave} (ft/d)	Computed (ft/d)
Rivers (RIV package)								
East Gallatin River								
EG1	0.03	283.5	40	1	1	11,340	5,671	11,340
EG2	0.03	283.5	40	1	1	11,340	5,671	11,124
EG4	0.03	283.5	41	1	1	11,624	5,812	11,624
EG5	0.03	283.5	48	1	1	13,608	6,805	9,179
EG6	0.03	283.5	50	1	2	14,175	7,088	11,391
EG7	0.03	283.5	53	1	2	15,026	7,514	4,532
EG8	0.03	283.5	47	1	1	13,325	6,663	13,027
EG9	0.03	283.5	78	1	2	22,113	11,058	206
Gallatin River								
GR1	0.03	283.5	73	1	2	20,696	10,349	20,696
GR2	0.03	283.5	60	1	2	17,010	8,506	12,073
GR3	0.03	283.5	68	1	2	19,278	9,640	2,834
GR5	0.03	283.5	48	1	1	13,608	6,805	1,477
GR6	0.03	283.5	101	1	3	28,634	14,318	18,314
GR	0.03	283.5	120	1	4	34,020	17,012	3,957
Hyalite Creek								
HY1	0.03	283.5	20	1	0.6	5,670	2,835	2,858
HY2	0.03	283.5	60	1	1.8	17,010	8,506	4,153
HY3	0.03	283.5	20	1	0.6	5,670	2,835	3,771
Drains (DRN package)								
Spaulding Brook	0.03	283.5	10	1	0.3	2,835	1,418	2,835
Gibson Creek	0.03	283.5	10	1	0.3	2,835	1,418	1,556
Cowan Creek	0.03	283.5	10	1	0.3	2,835	1,418	596
Story Creek	0.03	283.5	10	1	0.3	2,835	1,418	1,911
Ben Hart Creek	0.03	283.5	10	1	0.3	2,835	1,418	2,397
Bull Run Creek	0.03	283.5	10	1	0.3	2,835	1,418	1,874
Smith Creek (lower)	0.03	283.5	10	1	0.3	2,835	1,418	660
Thompson Creek	0.03	283.5	10	1	0.3	2,835	1,418	2,835

aquifer test in water-right application 41H 30029944 pumped at 103,950 ft^3/d for 72 h. A drawdown of 28 was measured in the pumped well and 4.5 ft was measured at the observation well during the aquifer test. The numerical model simulated a 3-ft drawdown at the pumping well, with a 2-ft drawdown at the adjacent observation well. The River Rock aquifer test (water-right 41H 102031 00) simulated pumping for 1 yr at a rate of 235,813 ft^3/d. Drawdown from this well was simulated at 8 ft, which is compared to the 36-ft drawdown measured during the test. At test site 255476, the simulated well pumped for 1 yr at a rate of 231,000 ft^3/d. The numerical model estimated approximately 6 ft of drawdown at the pumping well as compared to the 12 ft from the pumping test. Table A5 describes the aquifer test information and computed drawdowns from the numerical model.

These results are a reasonable calibration and representative of the aquifer at each location. The numerical model cell size causes the drawdown to appear muted as the calculated drawdown is dispersed over a 90,000 ft^2 area rather than at a point source (i.e., the well). The short-term testing (72 h) and the wide distribution of simulated pumping due to the cell size makes comparisons imperfect. The assumption that the

Table A4. Stream (DRN) elevations top and bottom of model nodes.

Drain Reach	Node #	GWIC ID[a]	Top Elev.	Bot Elev.
Bull Run Creek	1	262933	4,210.1	4,205.1
	2	—	4,324.8	4,319.8
Spaulding Brook	3	—	4,290.0	4,285.0
	4	—	4,220.4	4,215.4
Gibson Creek	5	262881	4,242.1	4,237.1
	6	—	4,348.8	4,343.8
Cowan Creek	7	—	4,325.5	4,320.5
	8	262901	4,247.6	4,242.6
Story Creek	9	—	4,255.7	4,250.7
	10	—	4,345.2	4,340.2
Ben Hart Creek	11	—	4,329.1	4,324.1
	12	—	4,297.1	4,292.1
Smith Creek	16	—	4,272.9	4,267.9
Smith/Reese Creek	21	264839	4,346.7	4,341.7
Reese Creek	20	—	4,390.1	4,385.1
Thompson Creek	22	264840	4,323.6	4,318.6
	28	—	4,441.3	4,436.3

[a]Locations correspond to nearest GWIC ID on stream locations are not exact to nodes.

Table A5. Superposition model simulated aquifer test conditions vs. actual site conditions.

Aquifer Test	Lat	Lon	depth	Discharge Rate (ft^3/d)	Aquifer Test Drawdown (ft)	Simulated Drawdown	Distance to 1 ft drawdown
STRD (GWIC ID 255476)	45.788	-111.2592	63	231,000	12	6	900–2,000
River Rock subdivision	45.7748	-111.2197	280	235,813	36	8	3,390–7,700
Water Right 41H30029944	45.8067	-111.2183	135	103,950	28	3	1,700

72-h test reached drawdown equilibrium is necessary for comparison to the model; however, the time frames are incompatible. The model represents monthly time steps that would not accurately show drawdown after only 3 days. Results that fall within the same order of magnitude and represent a reasonable distribution of the cone of depression are adequate for simulated results. The aquifer tests represent conditions at point sources in the aquifer, whereas the numerical model represents conditions throughout a much larger area. Two of the simulated tests (255476 and River Rock Subdivision) may have underestimated drawdown due to the proximity to the Gallatin River as the cone of depression extended out and pumping-induced river leakage.

An analytical model verified drawdown from pumping the transient 1-yr numerical model. The analytical model assumes a homogeneous aquifer with defined storage, transmissivity (based on aquifer thickness and hydraulic conductivity), and 365 days. The analytical model solves the Theis nonequilibrium method (Theis, 1935) with the Lohman (1979) well function modification.

The equation is as follows:

$$s(r,t) = \left(\frac{Q}{4\pi T}\right) W(u)$$

where s is aquifer storativity; (r, t) is drawdown at distance (r) at time (t) after the start of pumping; Q is discharge or pumping rate; T is aquifer transmissivity; and $W(u)$ is well function.

Table A6 shows the calculations in the analytical model and results of the 500,000 ft^3/d -pumping scenario. This table compares to figure A2 displaying the pumping-induced drawdown in the transient numerical model for the 500,000 ft^3/d pumping well at the River Rock subdivision (water-right 41H 102031 00). The numerical model cells are 299 ft and cell centered; therefore, the contour intervals should correspond to the analytical model at 299-ft distances. The numerical modeled contours indicate 9 ft of drawdown two cells from the pumping well, and 1-ft contours should occur near 12,750 ft from the well. In this case, induced river flow to the pumping well changes the cone of depression; however, the contours display within 1 to 2 ft of the predicted analytical model drawdown.

Table A6. Distance-drawdown tables estimated from the analytical model and results of the 500,000 ft^3/d -pumping scenario.

Aquifer storativity (s)	0.1	
Time (t)	365	day
Discharge (Q)	500,000	ft^3/day
Transmissivity (T)	28,000	ft^2/day

$$s(r,t) = \left(\frac{Q}{4\pi T}\right) W(u)$$

where s(r,t) represents the drawdown at distance (r) at time (t)

and W(u) represents the well function.

r (ft)	r^2	u	W(u)	Drawdown (ft)	Distance (ft)
300	90,000	0.00022	7.8442	11.1468	300
600	360,000	0.00088	6.4585	9.1778	600
900	810,000	0.00200	5.6487	8.027	900
1,200	1,440,000	0.00350	5.0749	7.2115	1,200
1,500	2,250,000	0.00550	4.6306	6.5802	1,500
1,800	3,240,000	0.00790	4.2683	6.0654	1,800
12,600	159,000,000	0.39000	0.7223	1.0264	12,600
12,900	166,000,000	0.41000	0.6907	0.9815	12,900

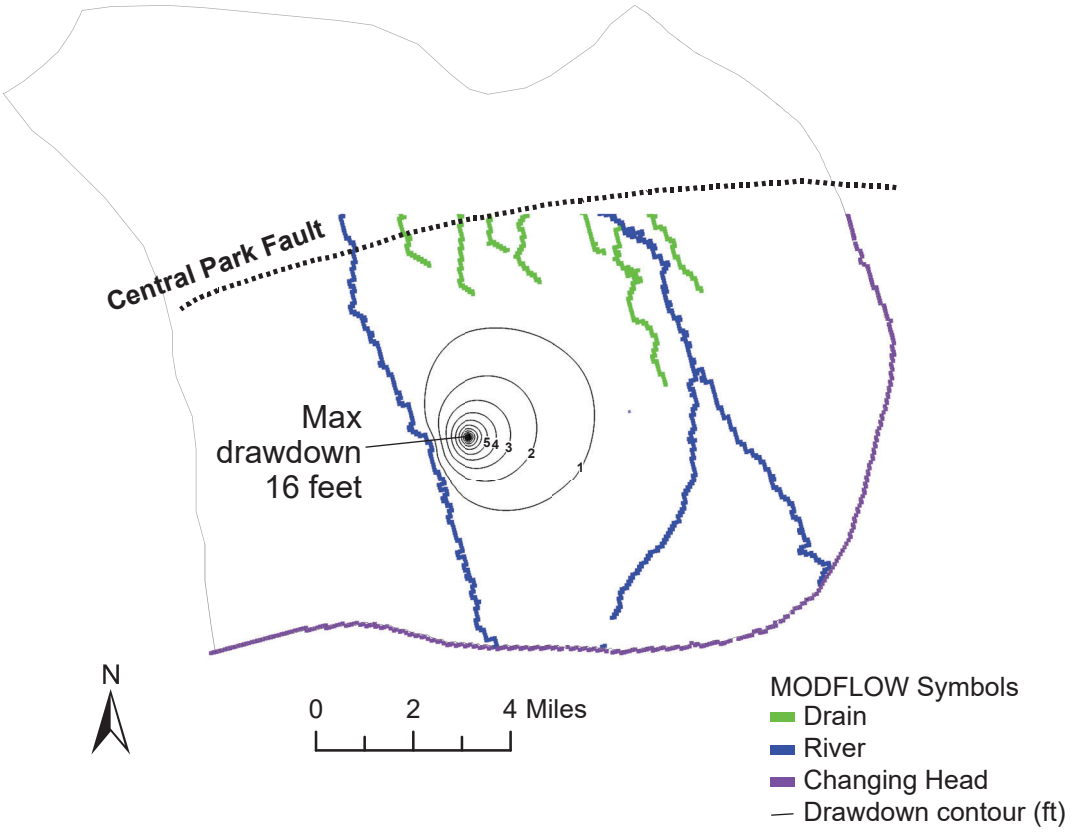

Figure A2. The pumping-induced cone of depression simulated in the numerical model for the River Rock subdivision (water-right 41H 102031 00). The model indicates the 1-ft drawdown contours should be reached at approximately 12,750 ft from the pumping well.